# Space weather and its relevance to Indonesia

Simon Wing

The Johns Hopkins University
Applied Physics Laboratory

# outline

1. What is space weather?
2. Space weather effects on satellite communication:
   a. polar region
   b. equatorial region
3. Space weather forecasting with machine learning
   - Kp forecast models
   - Solar cycle dependence of Kp forecasts
4. Summary

# 1. What is space weather?

# What is space weather?

Space weather refers to conditions on the sun, in solar wind, and in the Earth's magnetosphere, ionosphere, and thermosphere that can influence the performance and reliability of space-borne and ground-based technological systems and can endanger human life or health.

[The National Space Weather Program Strategic Plan, FCM-P30-1995, Washington D.C., 1995]

# Divisions of The Johns Hopkins University

**School of Arts & Sciences**

**Whiting School of Engineering**

**School of Professional Studies in Business & Education**

**School of Hygiene & Public Health**

**School of Medicine**

**School of Nursing**

**Applied Physics Laboratory**


**Nitze School of Advanced International Studies (SAIS)**

**Peabody Institute**

# JHU/APL & Space:

## *"From the Sun to Pluto -- and Beyond"*

since 1958:
64 spacecraft
150+ payloads

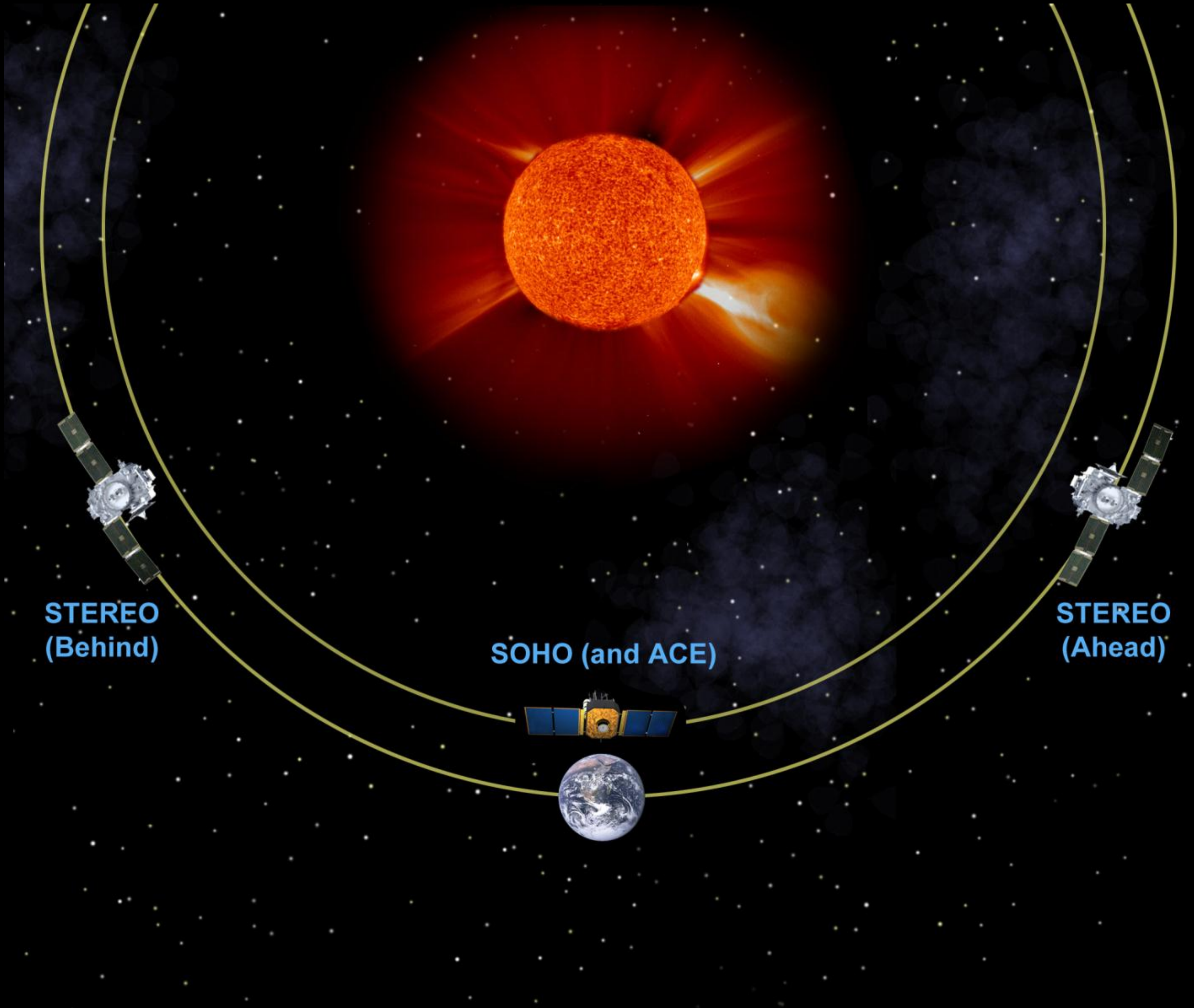


*STEREO spacecraft orbit generally along the Earth's orbit path. SOHO and ACE are about 1 million miles (1.6 km) towards the sun from Earth at the Lagrangian Point L1.*

Relative positions of SOHO & both STEREO spacecraft on November 24, 2009. STEREO will observe the entire Sun in early 2011.
(Diagram not to scale)

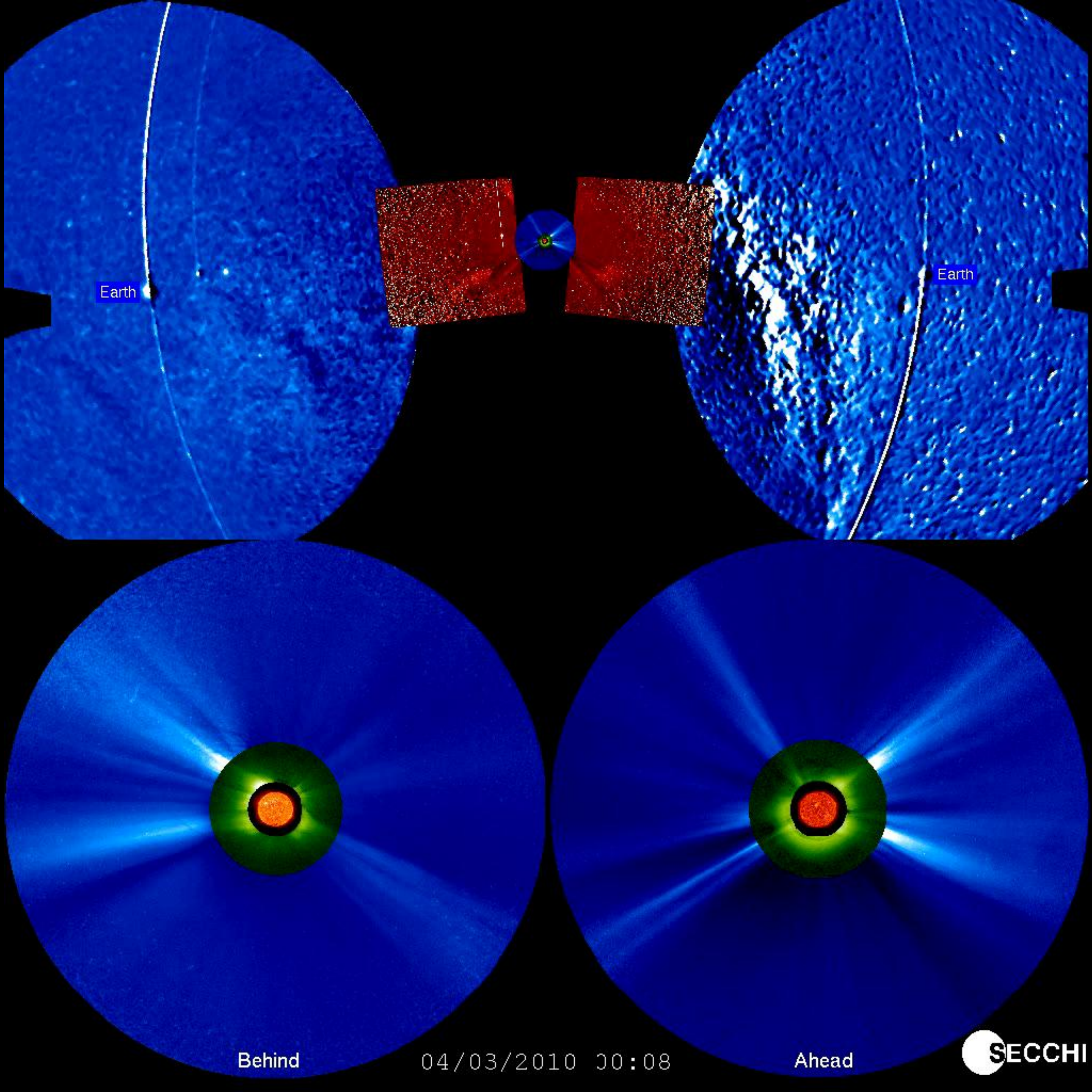
Earth
Earth
Behind
04/03/2010 00:08
Ahead
SECCHI

# some of the phenomena affected by space weather

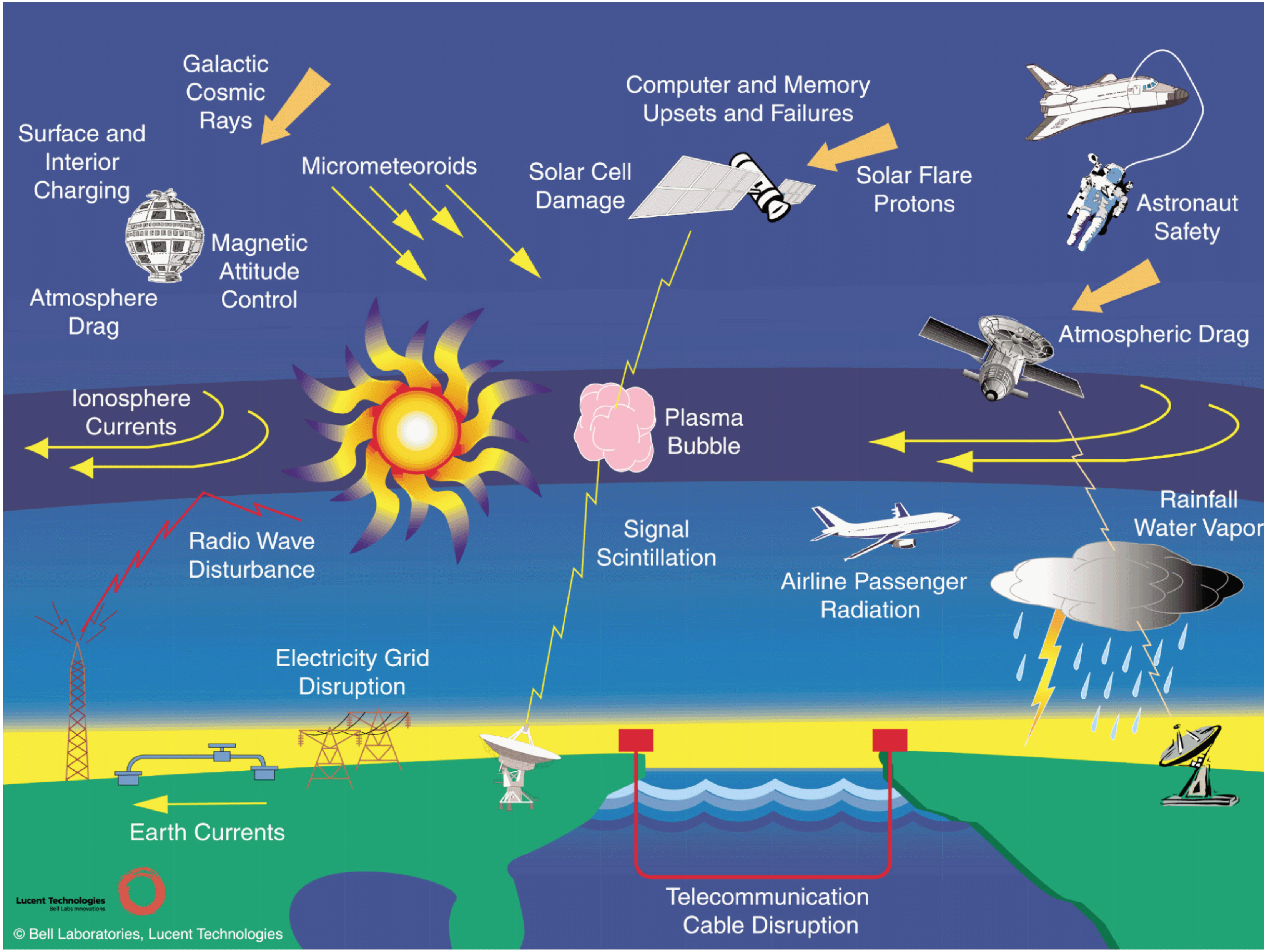

# Increasing reliance on space weather


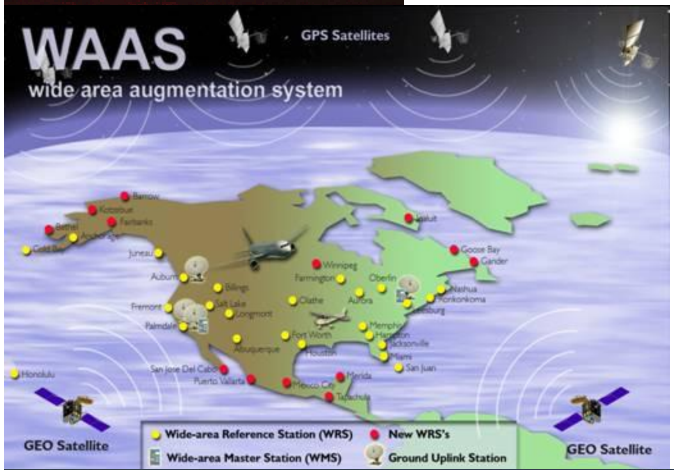




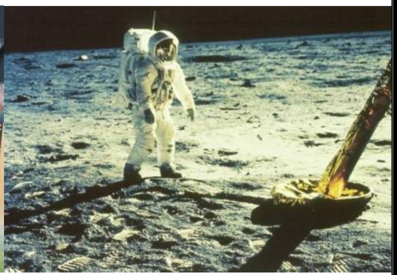

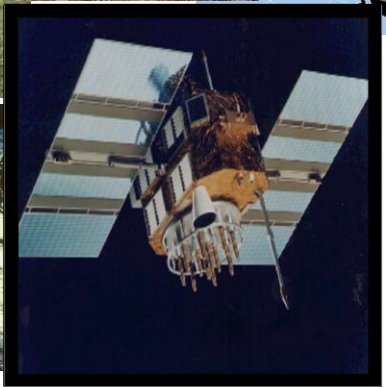

# Snapshot of some space weather products covering the region from the Sun to Earth

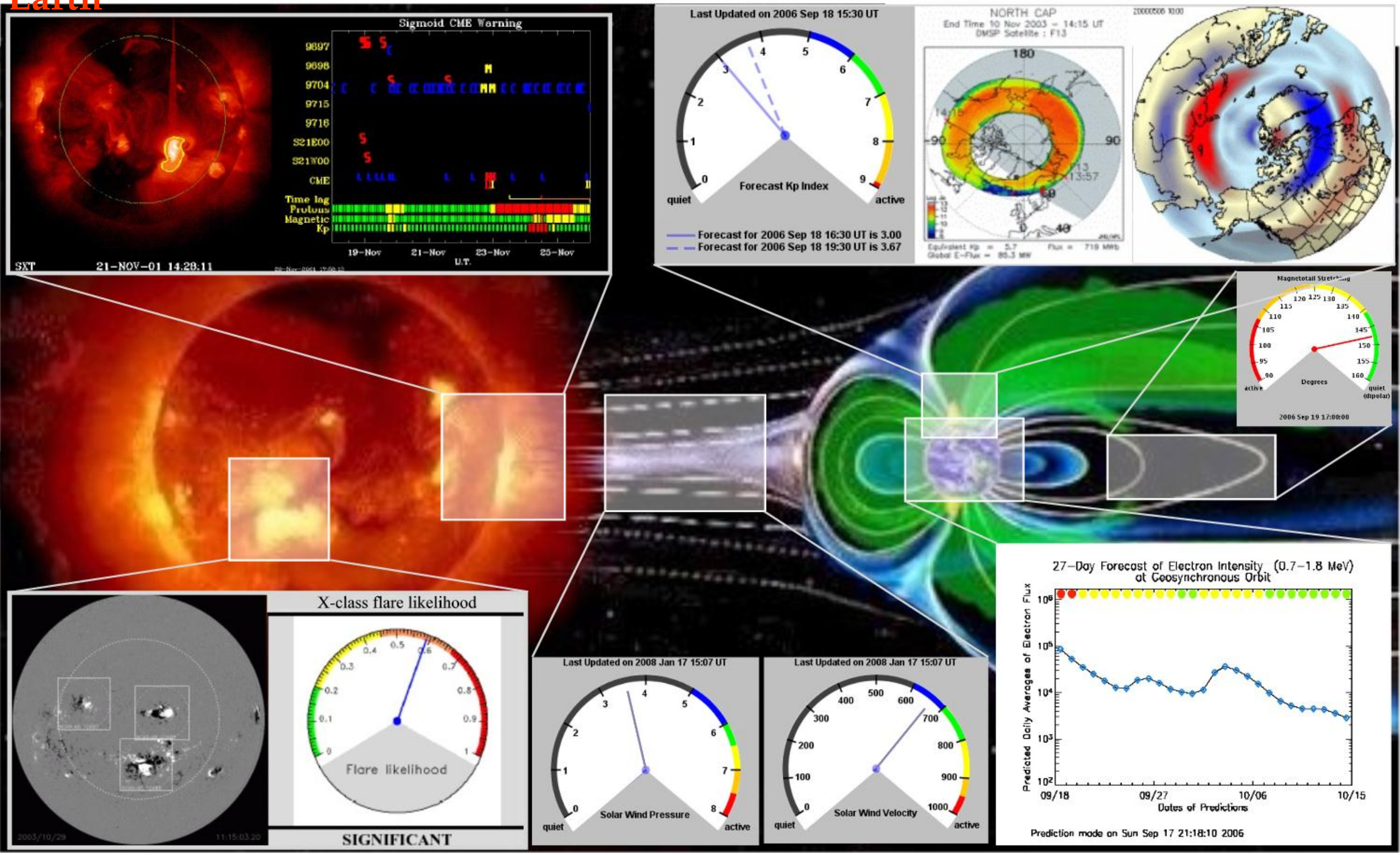

## Examples of space weather products that are available in realtime

| Region | Sub-region | Capabilities | Now cast | Fore cast | Lead APL scientists |
|---|---|---|---|---|---|
| The Sun | Photosphere | Major solar flare and CME prediction | √ | √ | M. Georgoulis |
| | Chromosphere | Ha filament identification | √ | | P. Bernasconi |
| | Corona | X-ray sigmoid identification / CME prediction | √ | √ | B. J. LaBonte/ M. Georgoulis |
| Solar Wind | near-Earth | IMF, solar wind density, velocity, pressure | | √ | ACE observations |
| Geospace | Near-Earth | Kp * # | | √ | S. Wing |
| | Near-Earth | Dst * | | √ | S. Wing |
| | Near-Earth/ Magnetotail | magnetotail stretching (b2i) | √ | | S. Wing/ P. Newell |
| Magnetosphere | Geosynchronous Orbit | 07-1.8 MeV & > 2 MeV electron fluxes * | | √ | T. Lui |
| | Radiation belt | Electron/proton fluxes & pitch angle at 2-8 Re * | √ | | M.-C. Fok/ Y.-H. Zheng |
| Ionosphere | High-latitude | size, position, intensity of auroral oval (OVATION) * | √ | | P. Newell |
| | High-latitude | intensity & location of field-aligned currents * | √ | | B. Anderson |

* Product has been transitioned to AFWA    # Product is being transitioned to NOAA and AFRL

# Radiation Belt Storm Probes (RBSP)

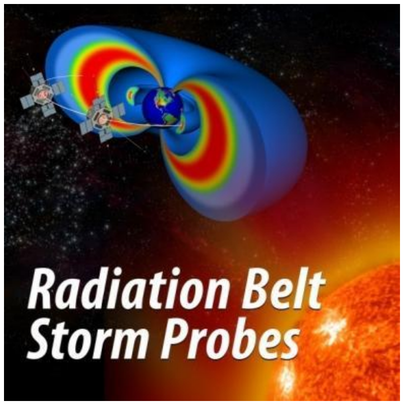


Objective:

Provide understanding, ideally to the point of predictability, of how populations of relativistic electrons and penetrating ions in space form or change in response to variable inputs of energy from the Sun.

Impacts:

1. Understand fundamental particle radiation processes operating throughout the universe.
2. Understand Earth's particle radiation belts and related regions that pose hazards to human and robotic explorers.

**a huge space weather component**

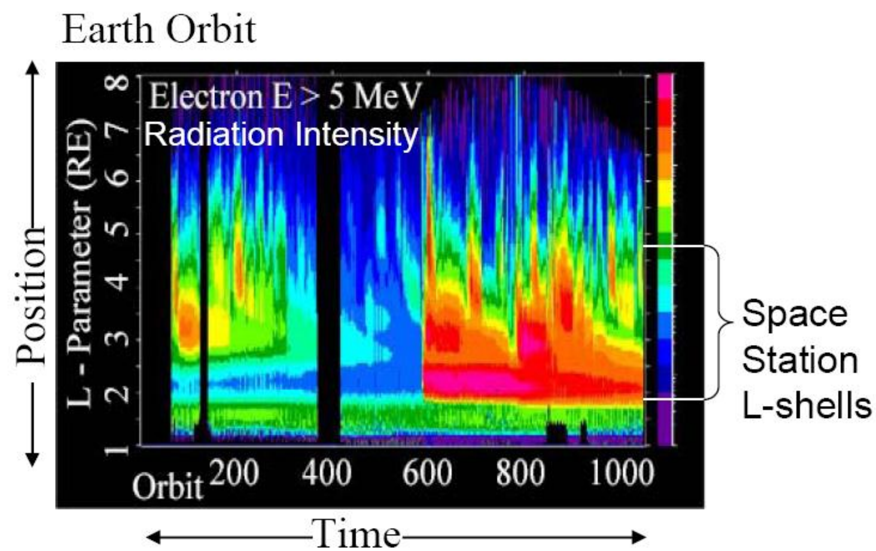


Intensities of Earth's dynamic radiation belts

# RBSP launched Aug 30, 2012

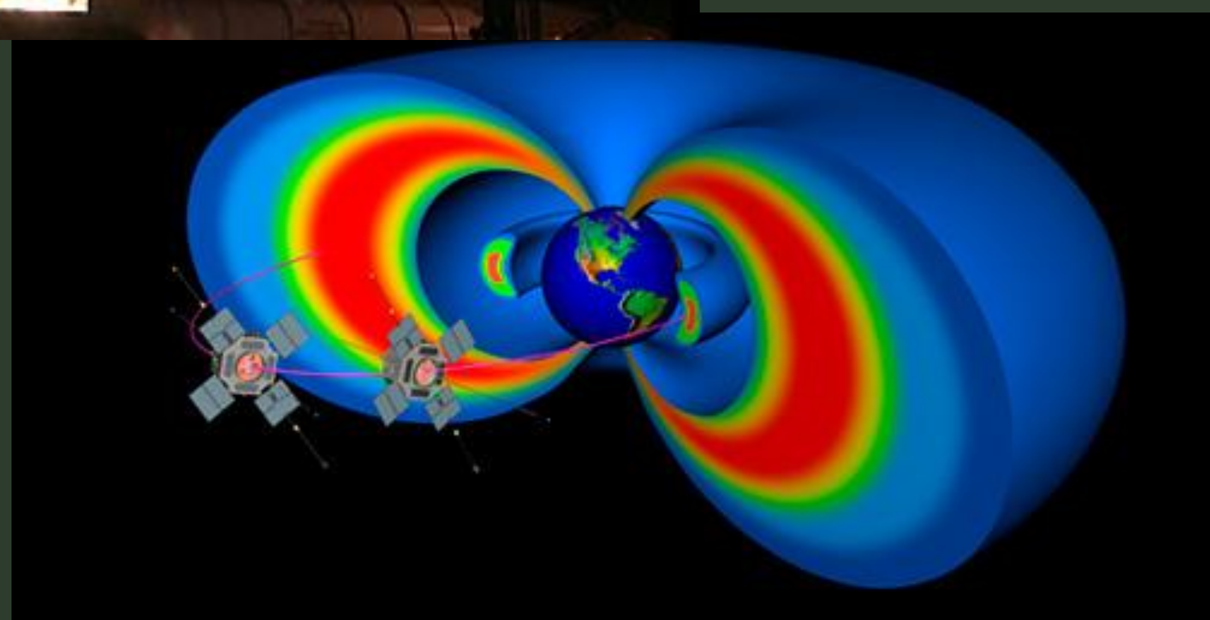

# Spacecraft charging

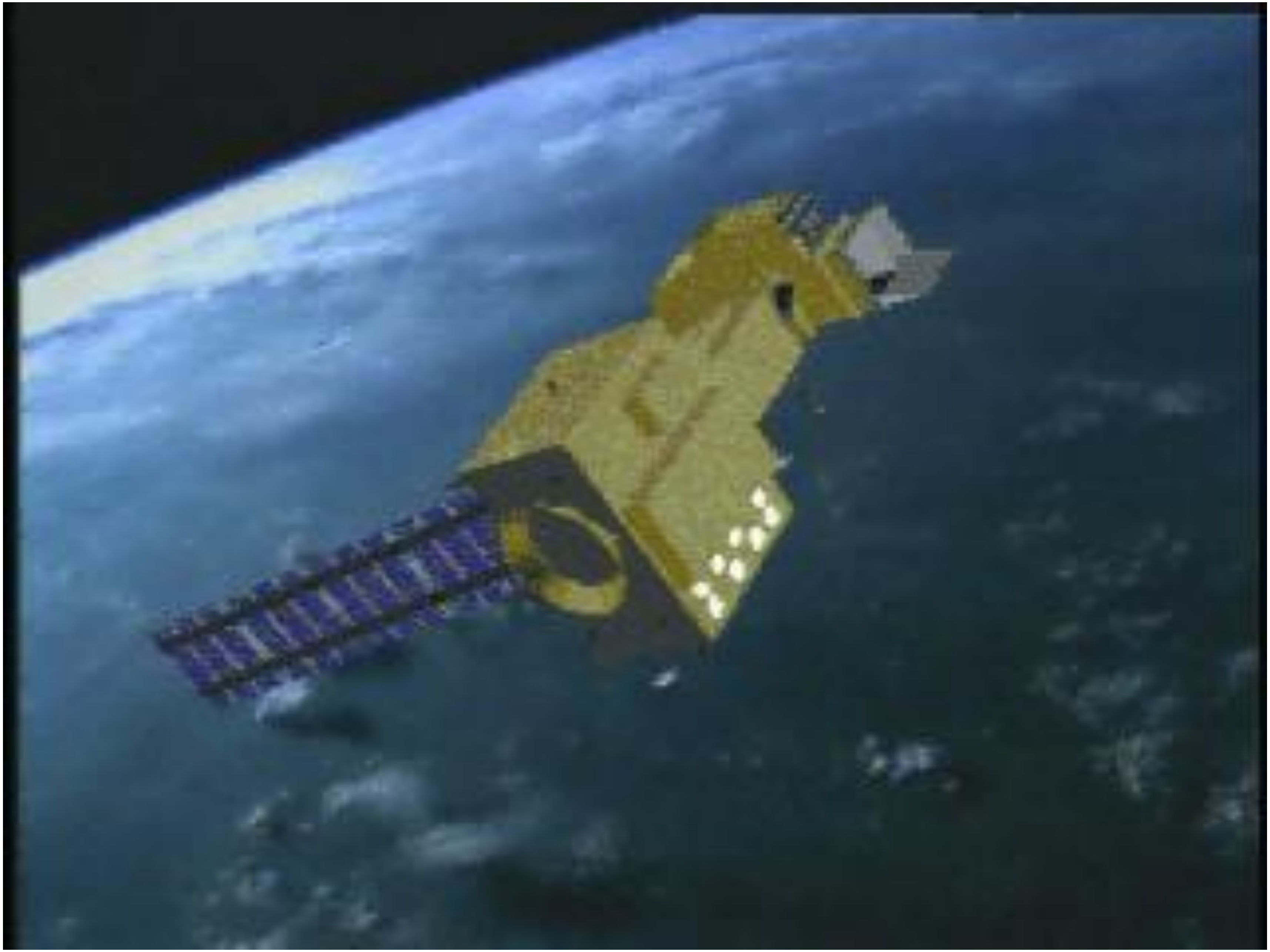

# Space weather research

- **Most space weather research traditionally has focused on high latitude phenomena**
- **There are still a lot of unknowns at low latitude**
- **There are lots of opportunities for country like Indonesia to contribute**

# 2. Space weather effects on satellite communication

a. Polar region
b. Equatorial region

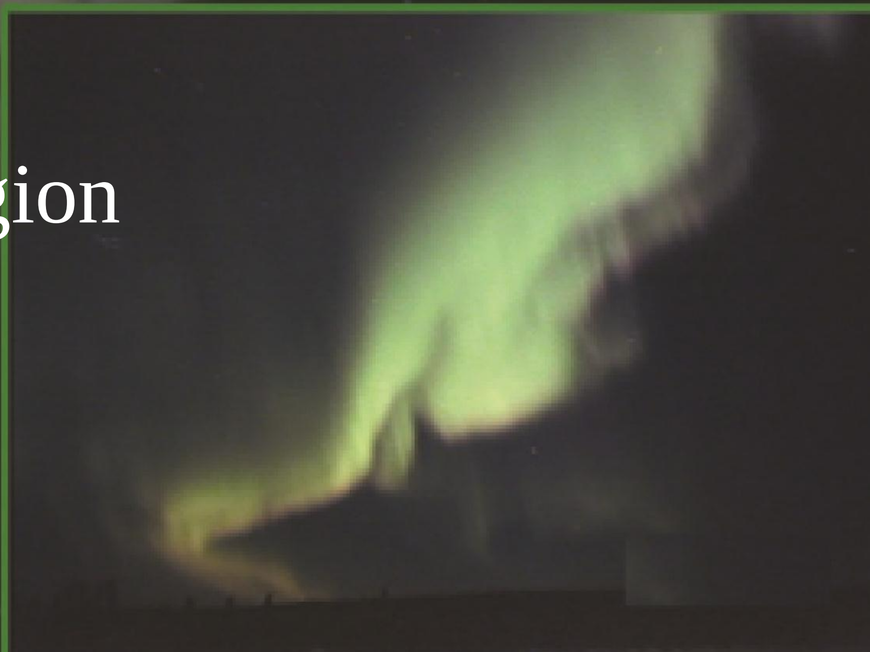

# Motivations

- GPS is now widely used all over the world, including Indonesia
- Indonesia has owned Palapa series communication satellites for almost 4 decades

PALAPA-B Satellites

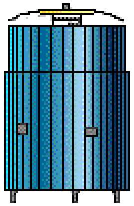

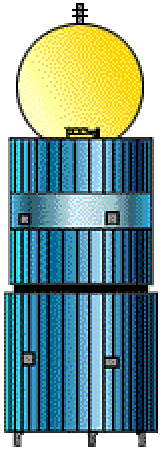

- Palapa-B covered equatorial region
- Owned by Indonesia's state-owned telecommunications company, TELKOM

# One-Way VSAT

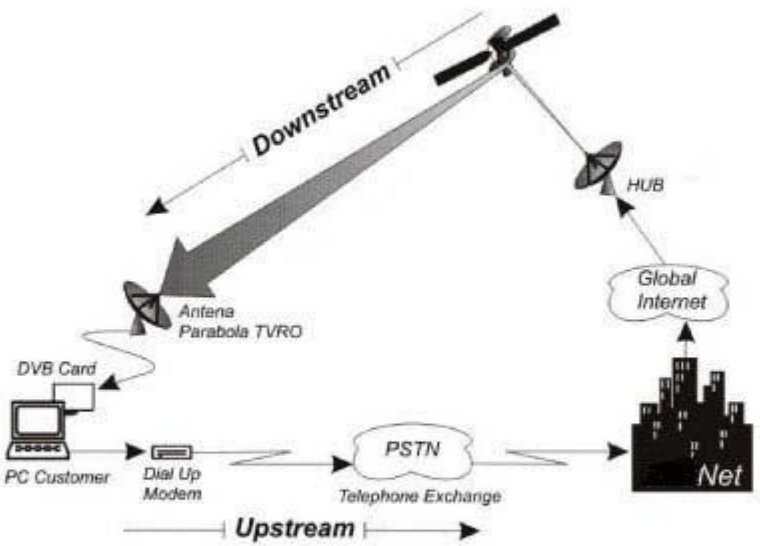


- Using technology like VSAT, Palapa can provide communication in remote and rural areas

# Two-Way VSAT

- Useful for education in areas without phone lines

# PALAPA-C

Palapa-C can cover equatorial and polar region

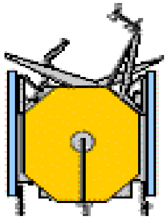

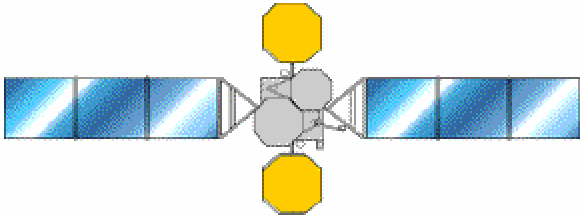

- C1 Launched Jan 1996, C2 Launched May 1996
- Unfolds to 21m in length, Solar panals provide 3700 W of power
- Still in service today

# PALAPA-C Coverage

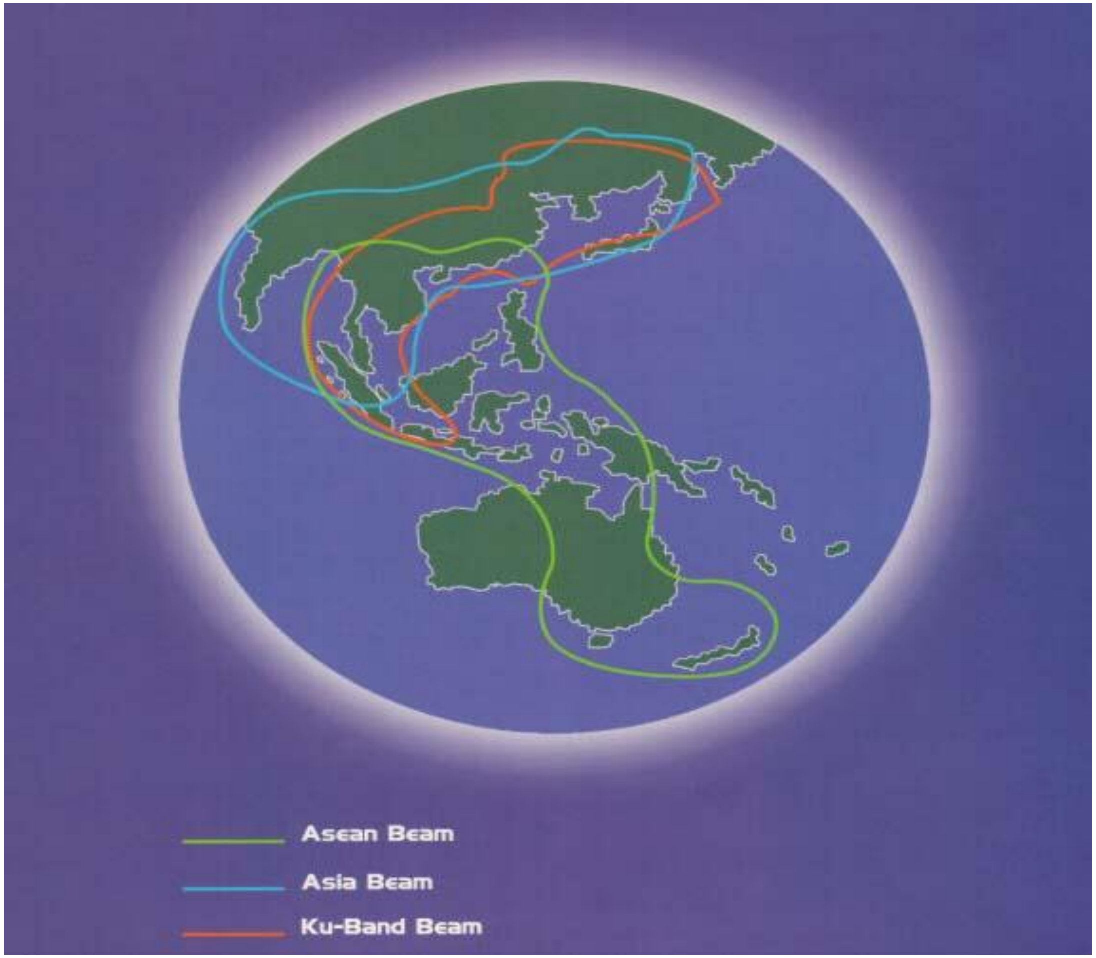


Palapa-C covers a wider geographical area, including polar region such as Southern Australia and New Zealand, which has its own challenges

# Two primary ionospheric regions that can disrupt satellite communications:

a. Polar region: auroral particle precipitation
b. Equatorial region: plasma bubble

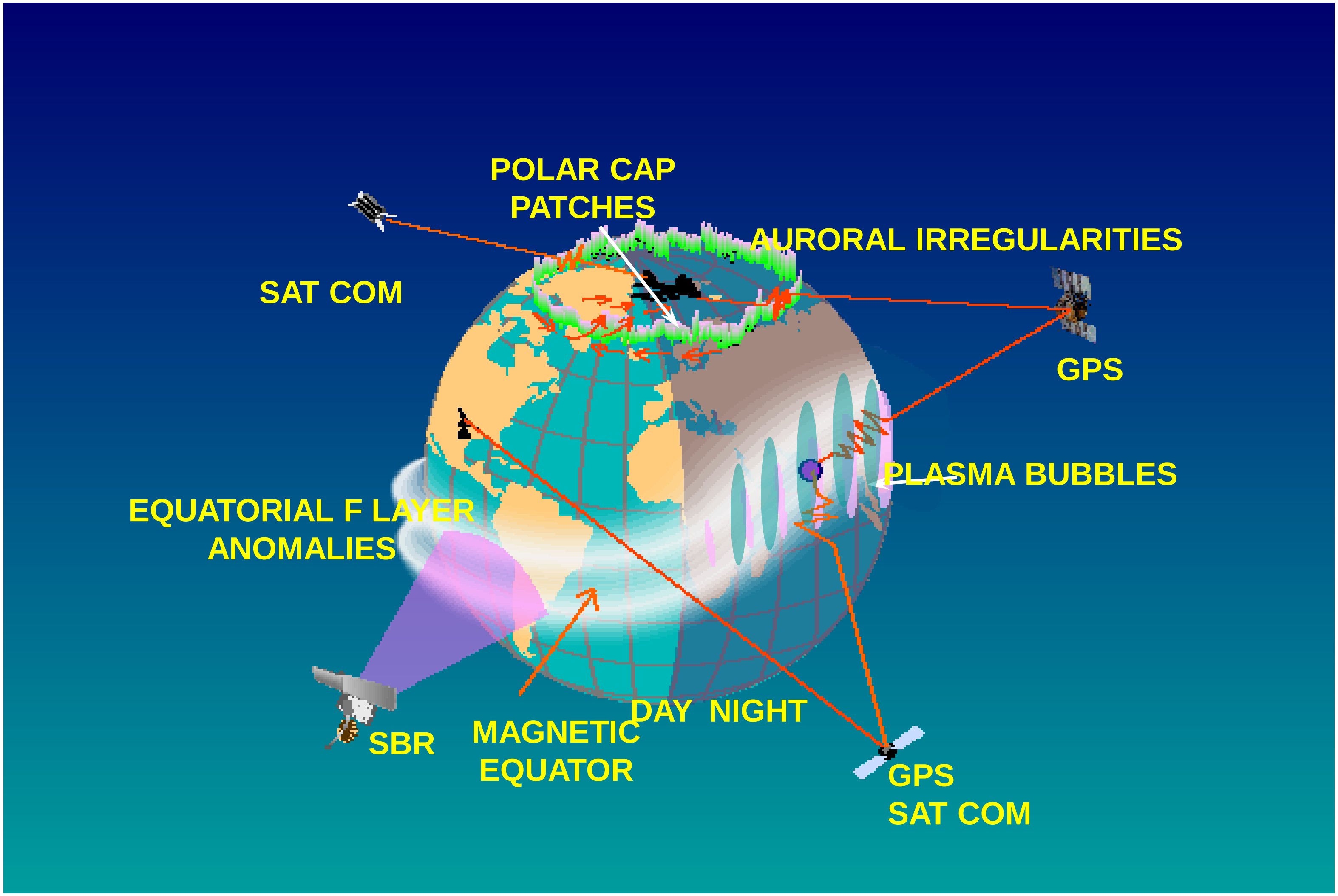

# Scintillation

## The Problem

- Ionospheric density gradients can distort satellite communication or radar signal traversing it to/from a satellite or target

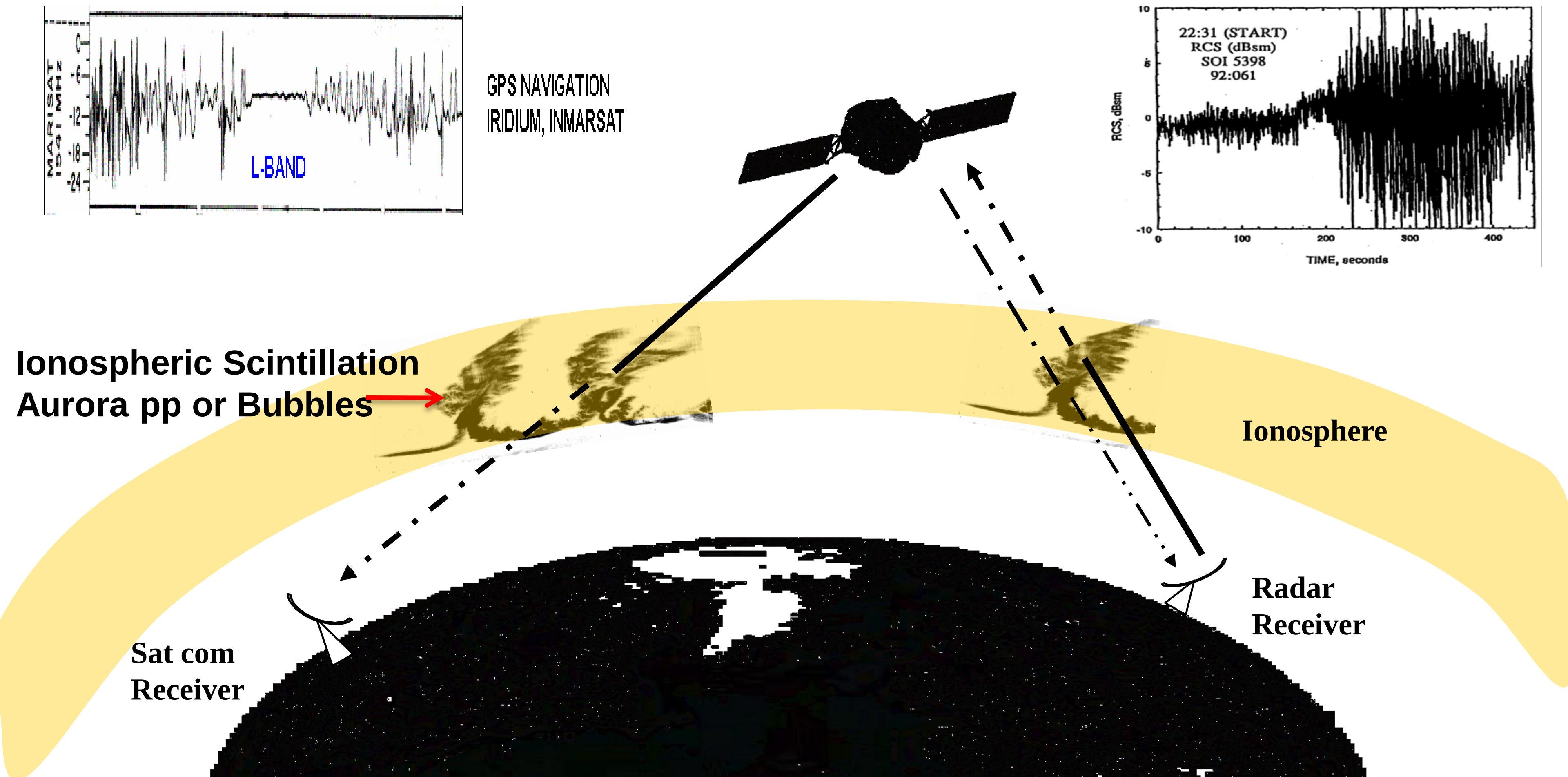

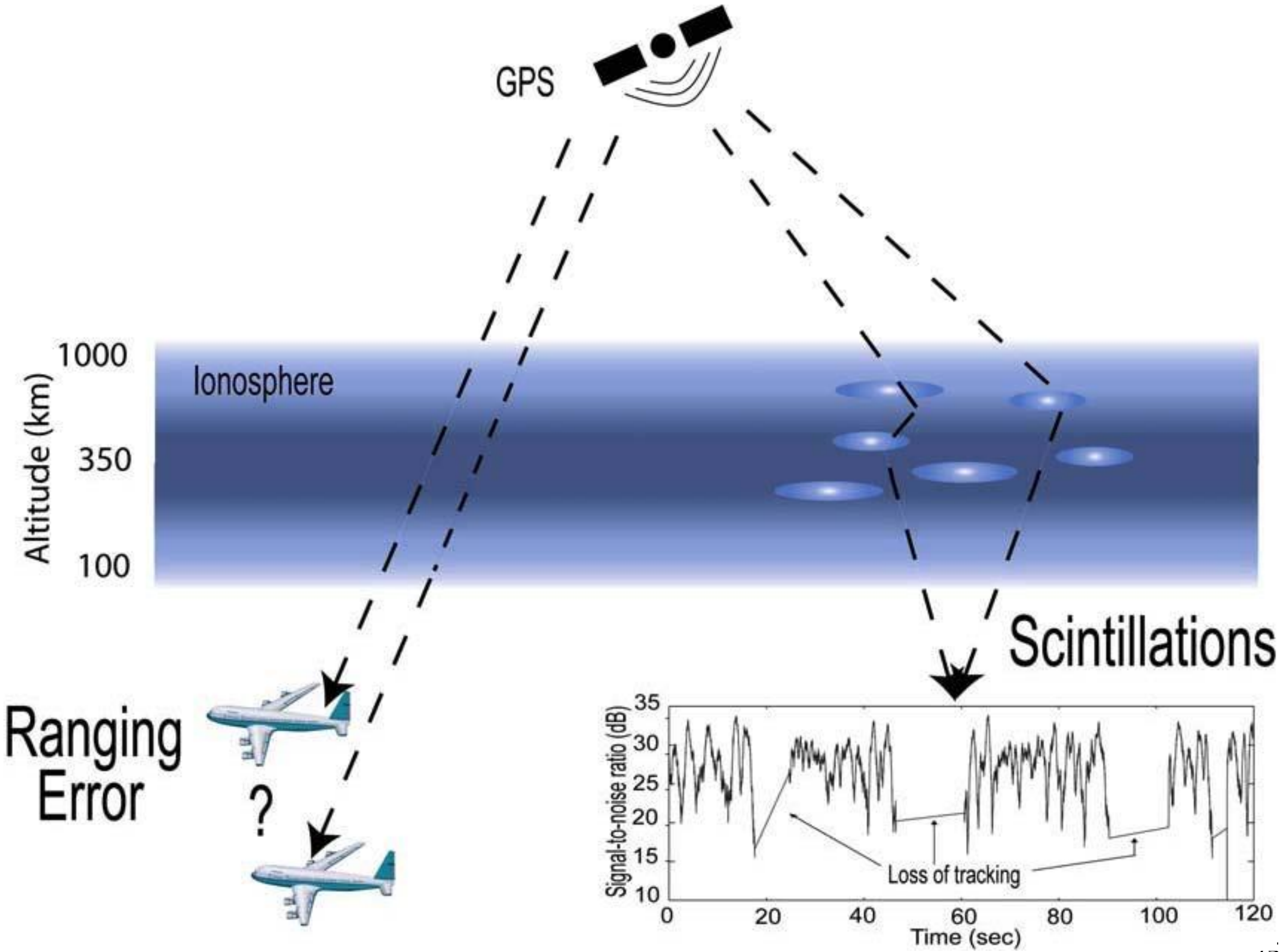

GPS
1000
Altitude (km)
350
100
Ionosphere
Scintillations
Ranging
Error
?
Signal-to-noise ratio (dB)
35
30
25
20
15
10
Loss of tracking
0
20
40
60
80
100
120
Time (sec)

## 2. Space weather effects on satellite communication

### a. Polar region: Auroral particle precipitation

# Aurora

vicinity of Fairbanks, Alaska (by Jan Curtis)

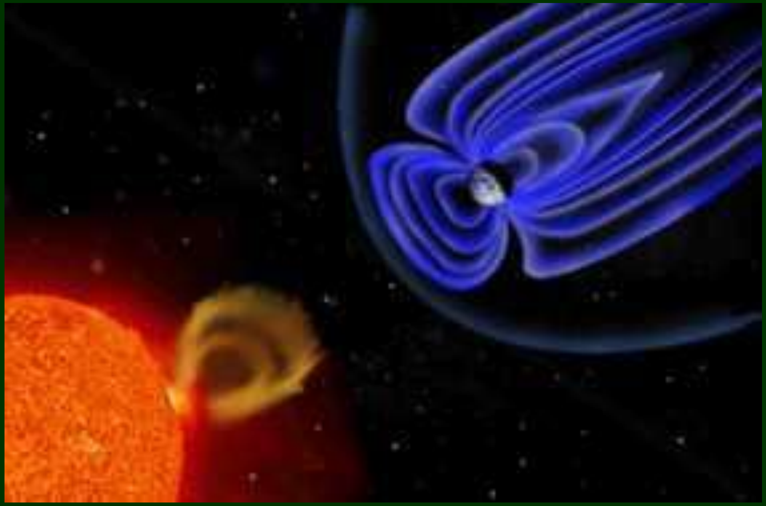

The Earth has a “halo” above north and south pole that is known as auroral oval

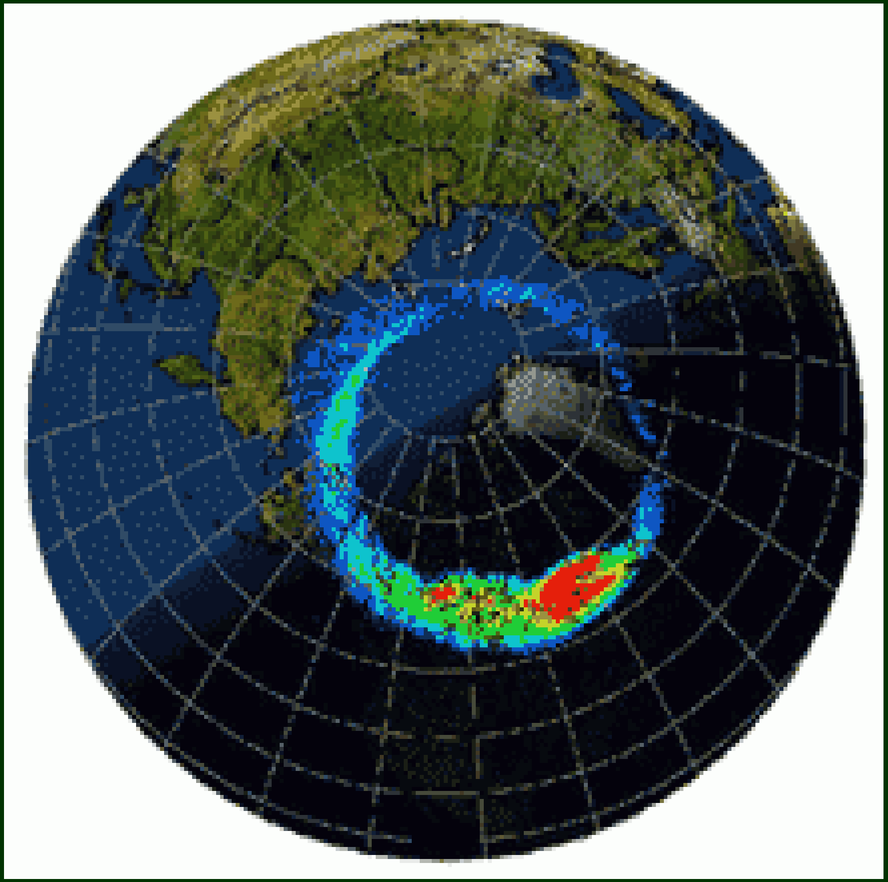

- Aurora is related to the activities of the Sun
- Aurora is an ionospheric emission due to particle precipitation
- The particles originate from the sun or/and magnetotail and follow the magnetic field line to the ionosphere

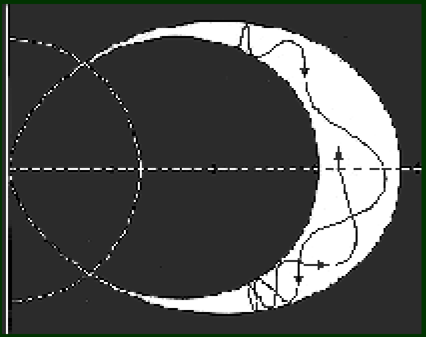

UV image of auroral oval (in false colors)

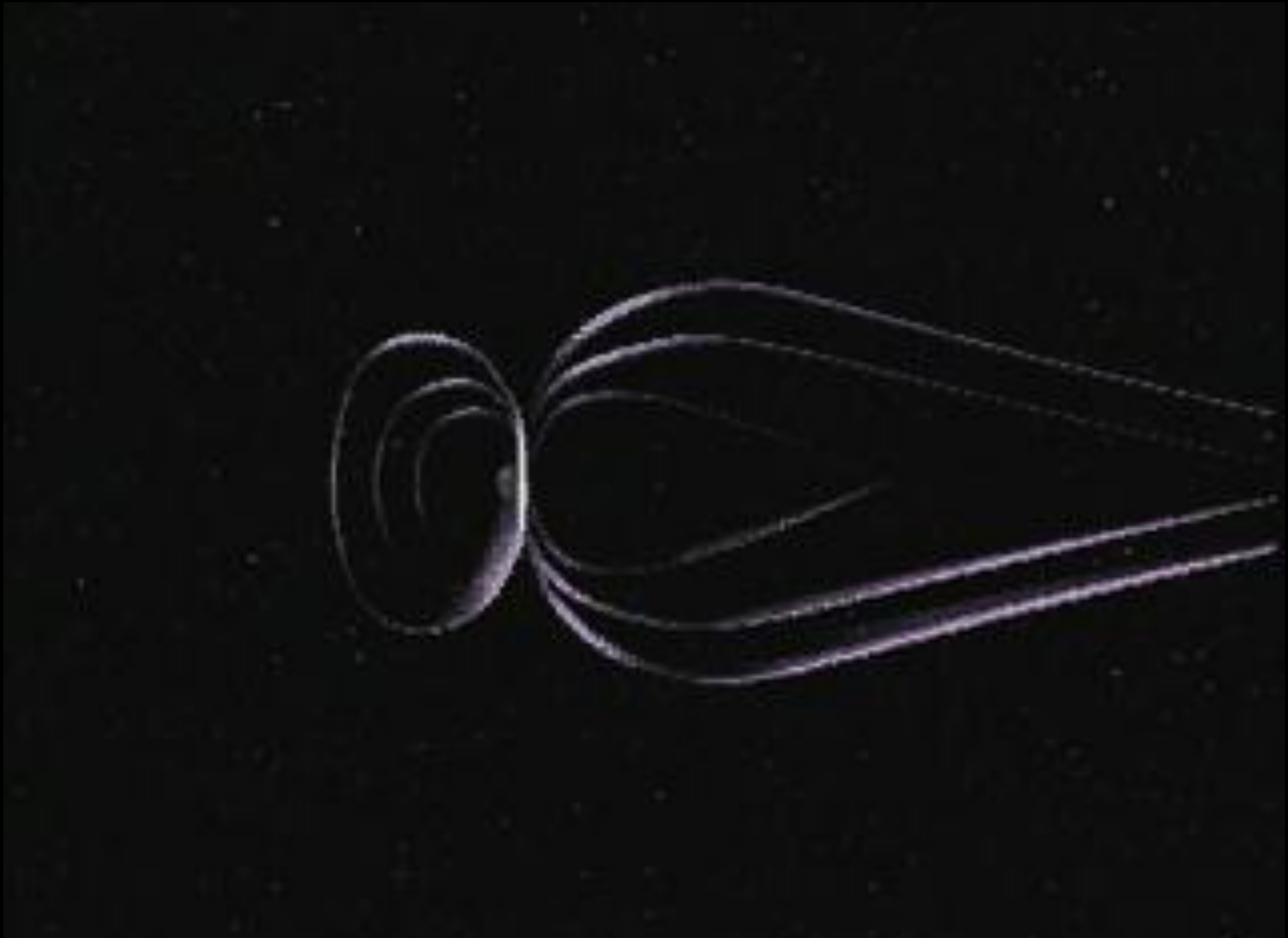

# The aurora seen from space

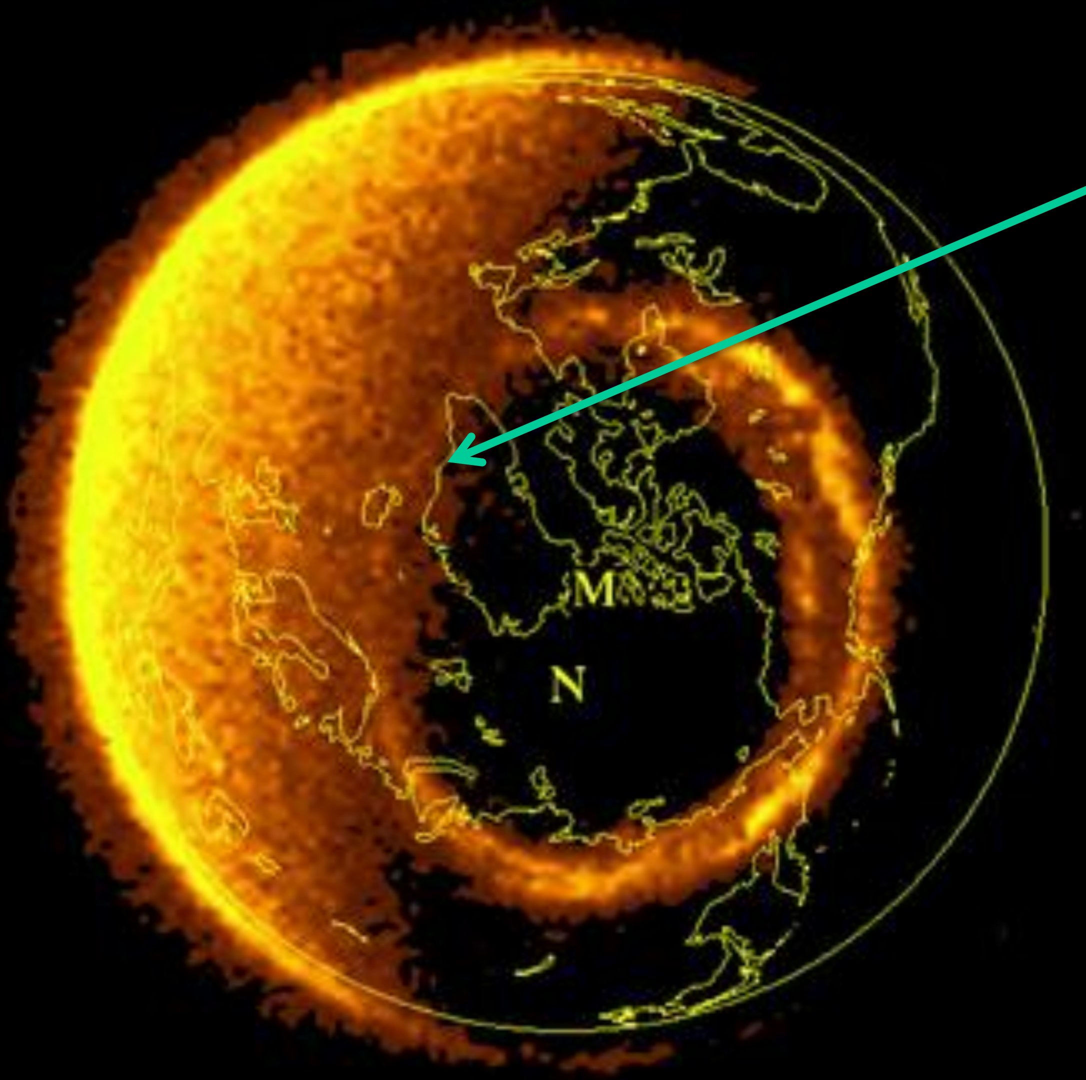


on the dayside aurora is harder to see

# aurora dynamics shown in movie taken from space

# Global MHD simulations showing aurora dynamics

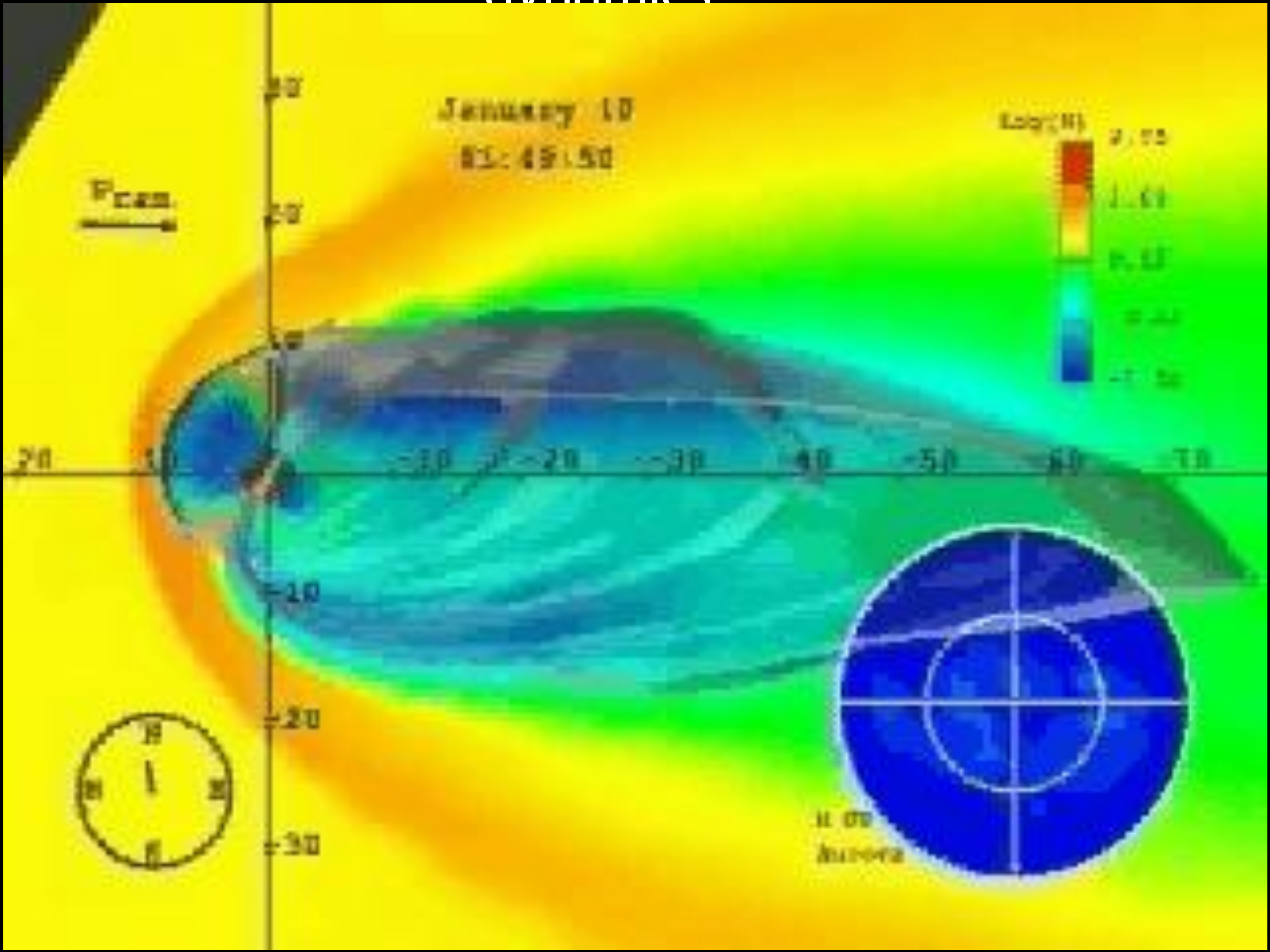

# Northern and Southern light

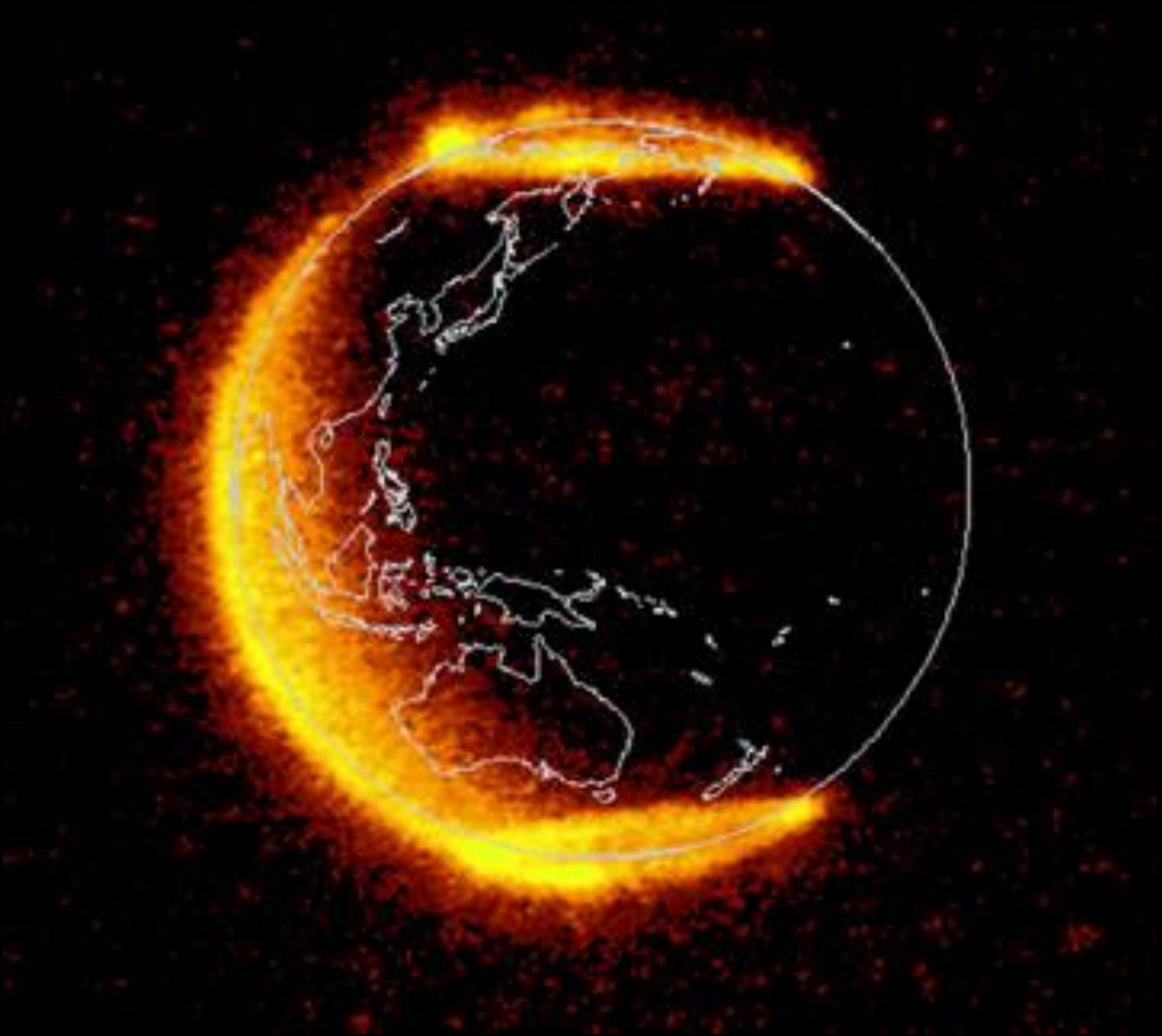

# (Auroral) Oval Variation, Assessment, Tracking, Intensity, and Online Nowcast (OVATION)

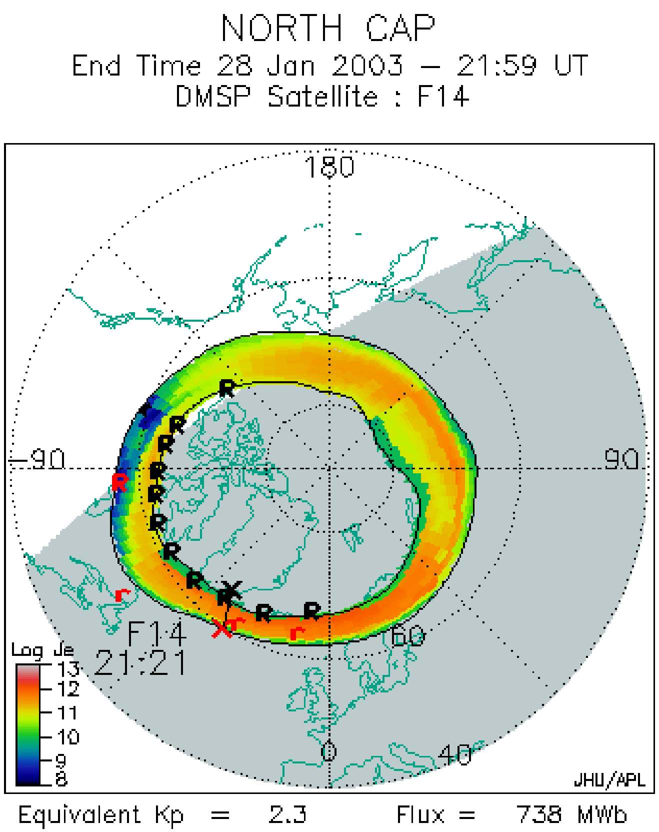


Newell et al. [2005]

X : DMSP boundaries

R : SuperDARN boundaries

P: MSP boundaries

r : SuperDARN upper-limit of the equatorward boundary position.

Intensity scale: log10 eV/cm2 s str.

Input:

DMSP SSJ4, UAF Meridian Scanning Photometer (MSP), SuperDARN radar

Output

Auroral oval location and intensity for both the northern and southern hemispheres, polar cap fluxes

inform possible communication problems, especially during active time

SW affects air travel

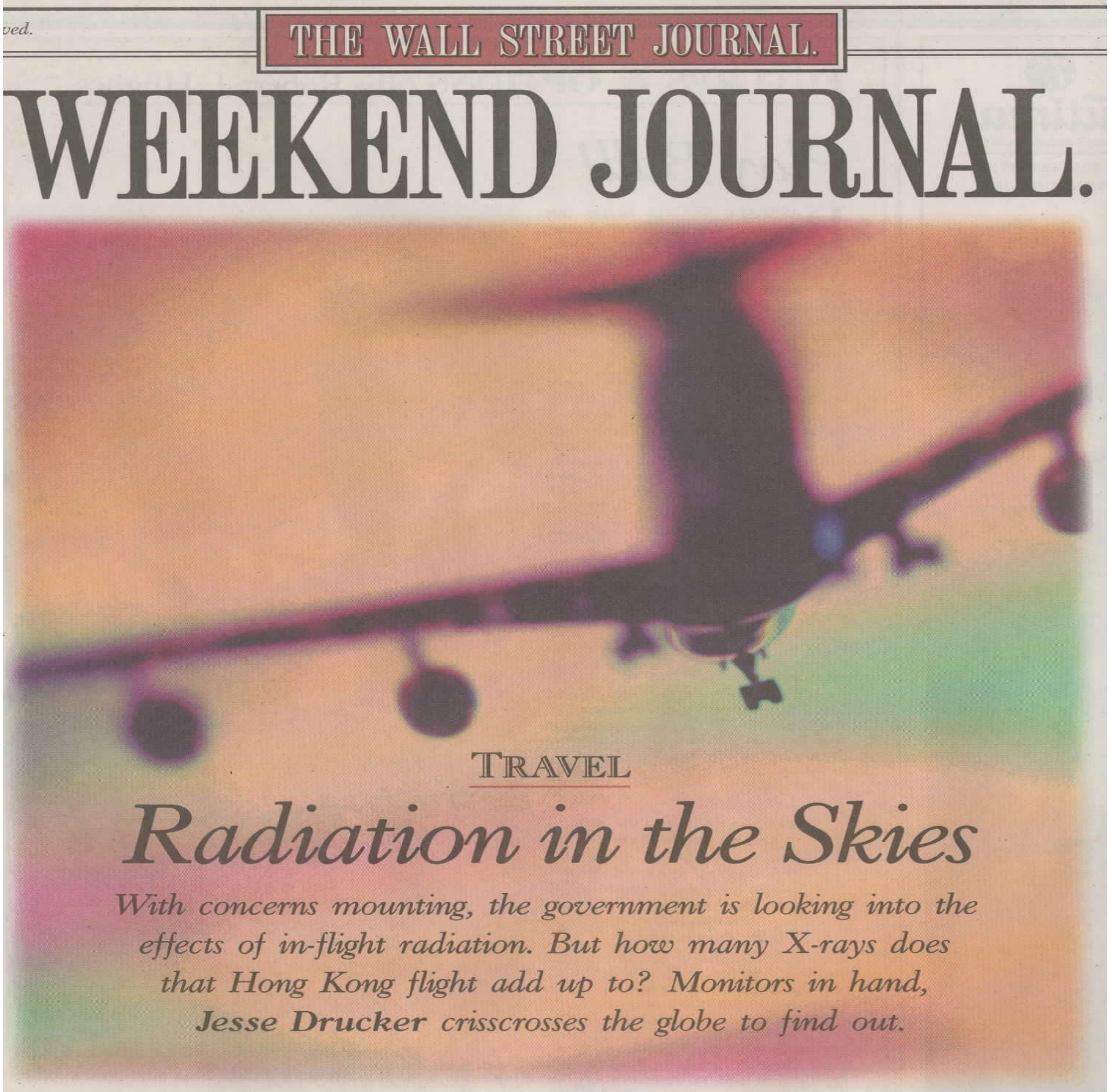

THE WALL STREET JOURNAL.

# WEEKEND JOURNAL.

TRAVEL

## *Radiation in the Skies*

*With concerns mounting, the government is looking into the effects of in-flight radiation. But how many X-rays does that Hong Kong flight add up to? Monitors in hand,* ***Jesse Drucker*** *crisscrosses the globe to find out.*

# United Airlines Polar Routes 2005

The airline diverts the travel path

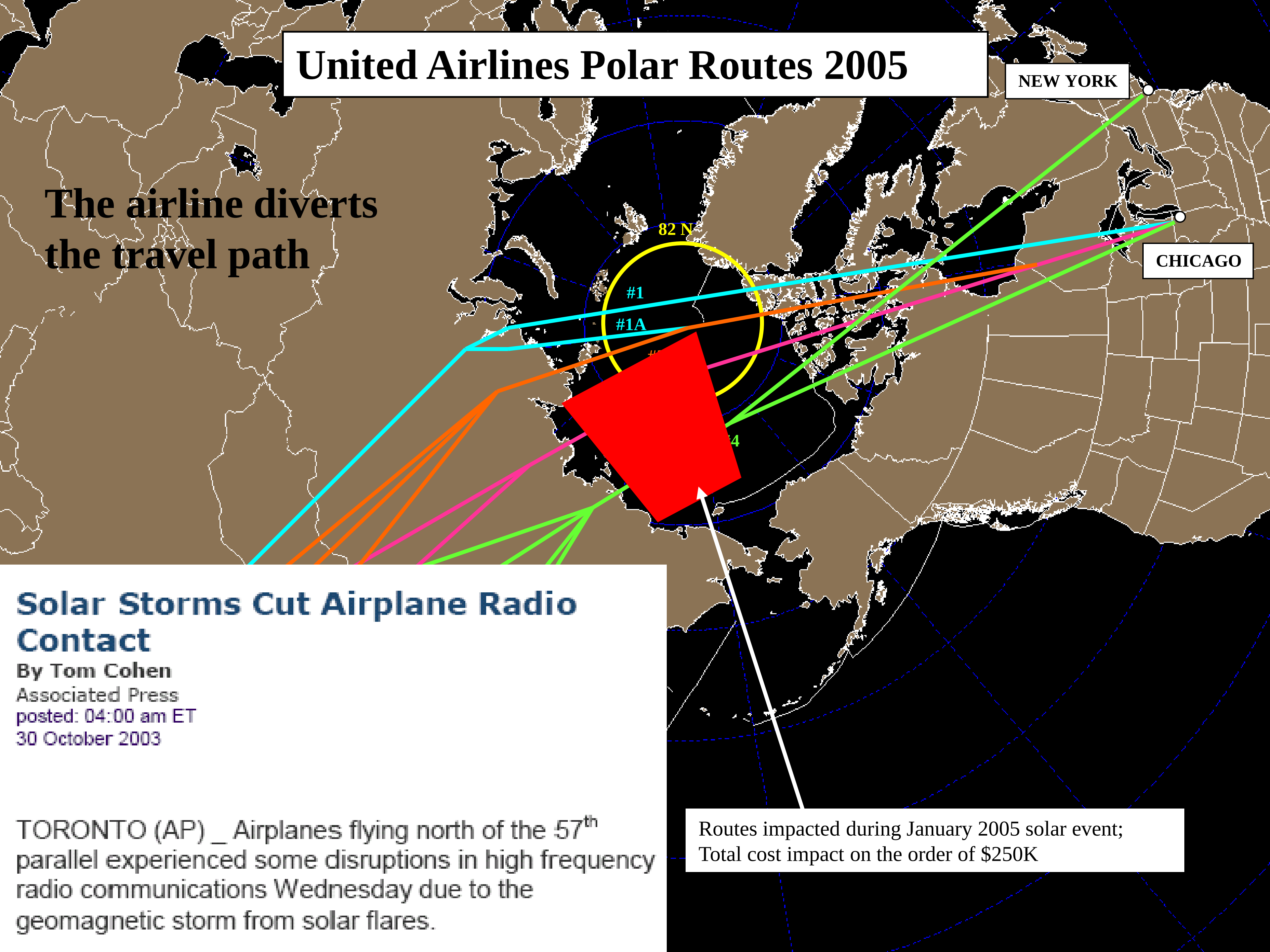


Routes impacted during January 2005 solar event; Total cost impact on the order of $250K

## Solar Storms Cut Airplane Radio Contact

**By Tom Cohen**
Associated Press
posted: 04:00 am ET
30 October 2003

TORONTO (AP) _ Airplanes flying north of the 57th parallel experienced some disruptions in high frequency radio communications Wednesday due to the geomagnetic storm from solar flares.

# Airline Radiation Exposure

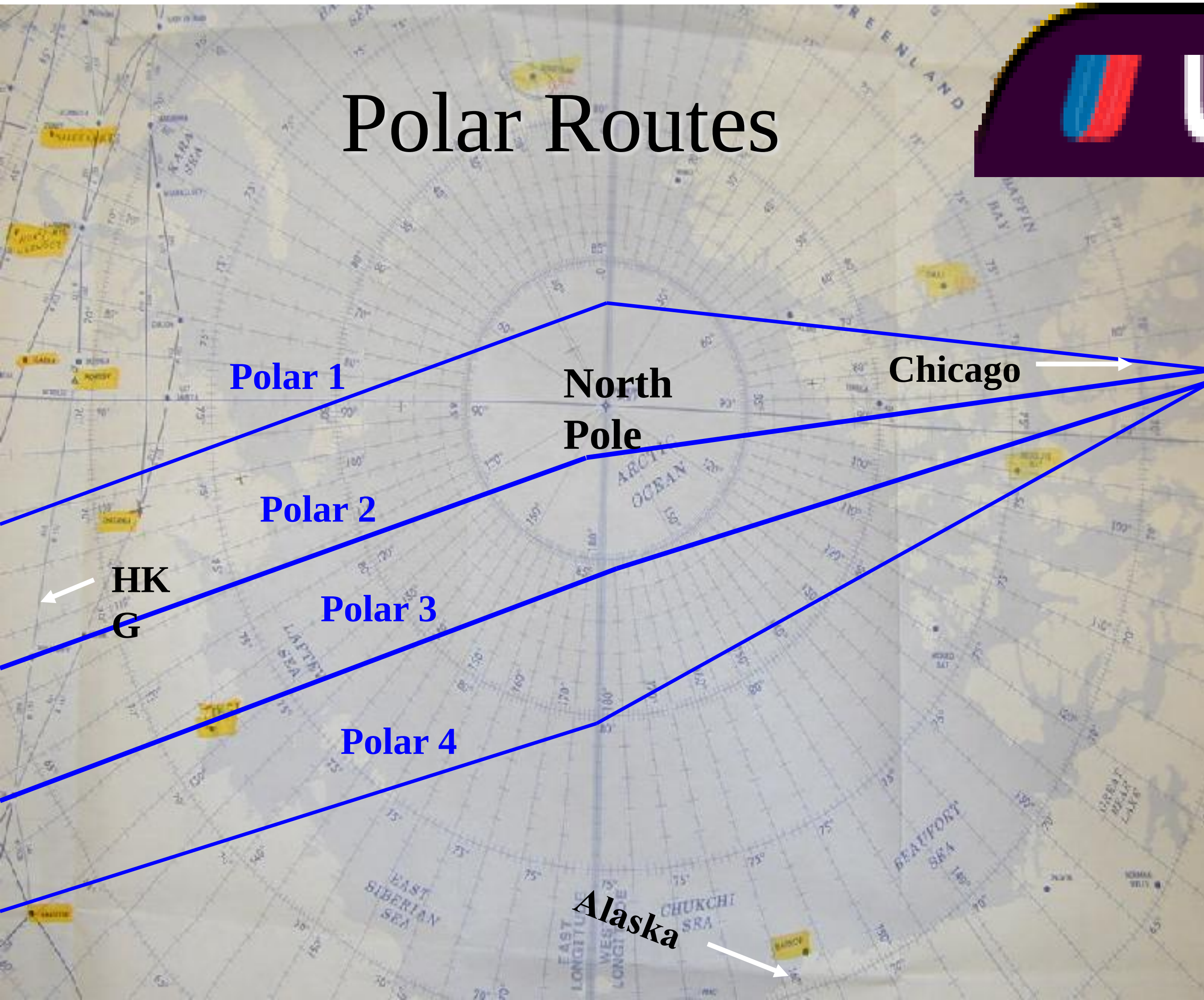


**Space weather predictions vital for radiation exposure, communications**

**Route selection based on prediction**

2. Ionospheric regions that can disturb satellite communication

b. Equatorial region: plasma bubble

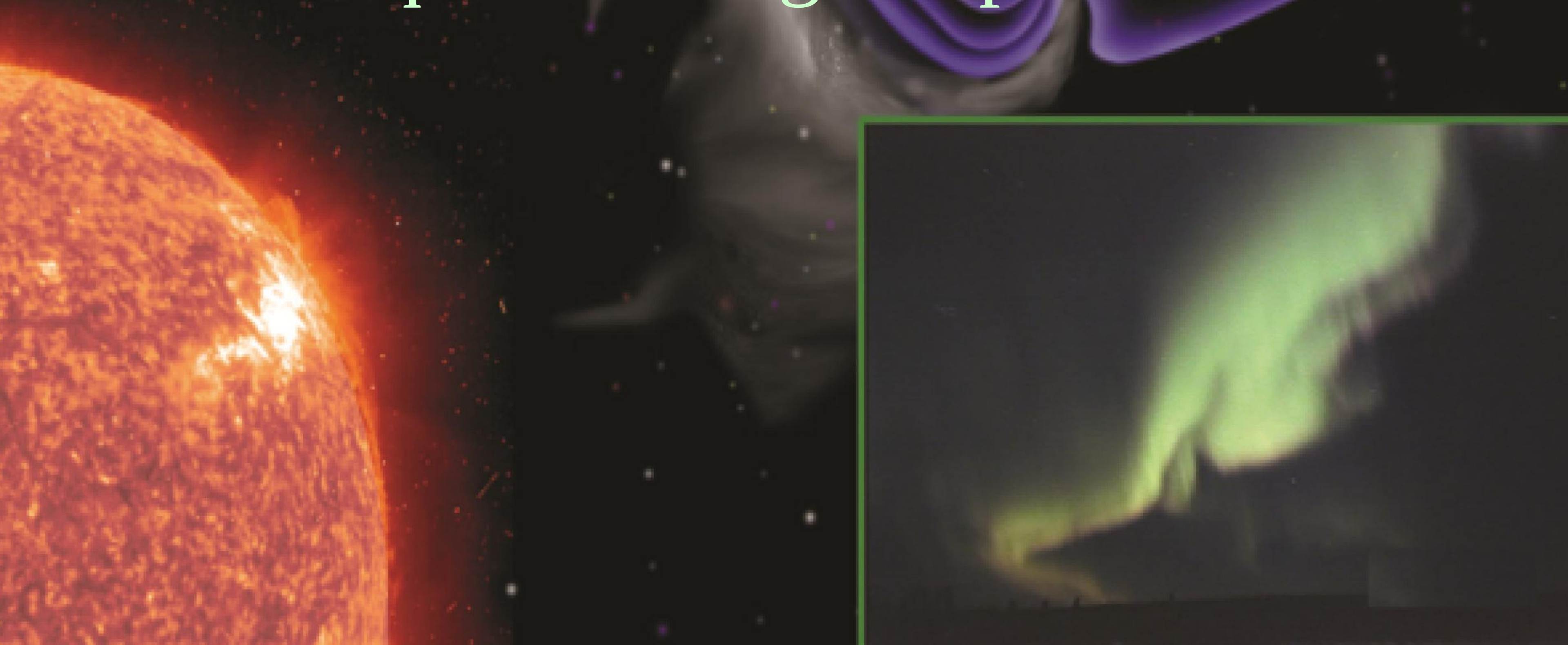

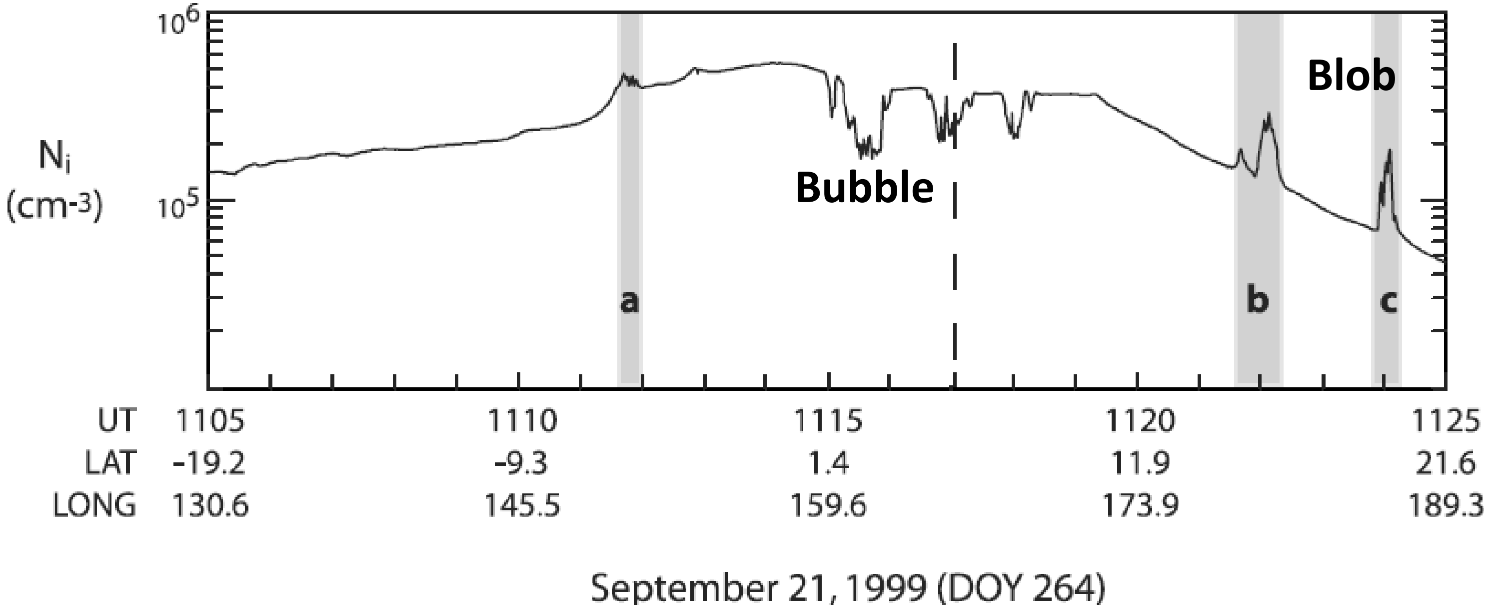


***Figure.*** *Sample plots of bubbles and blobs observed by ROCSAT-1 [Le et al., 2003]. Plasma bubbles and blobs are the local plasma density reduction and enhancement, respectively, relative to the background.*

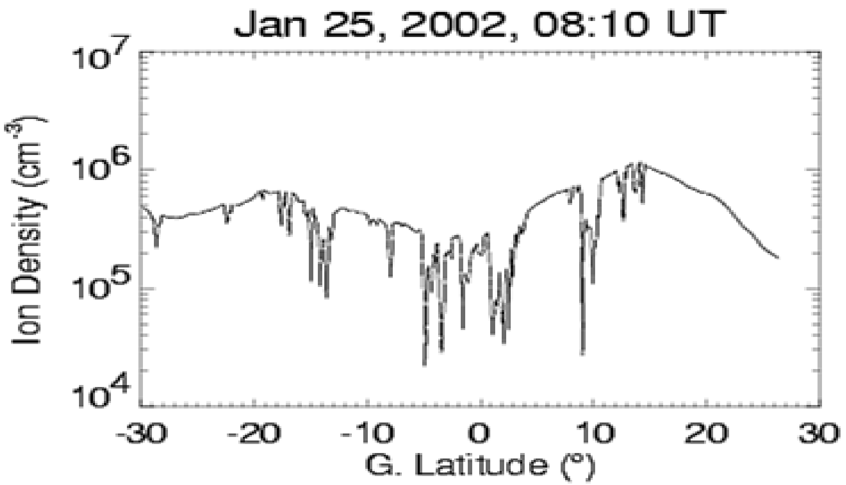


In-situ ion density measurements
at 600 km from the ROCSAT satellite

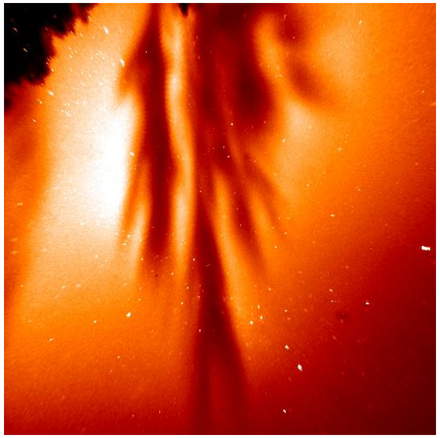

All-sky image in Brazil

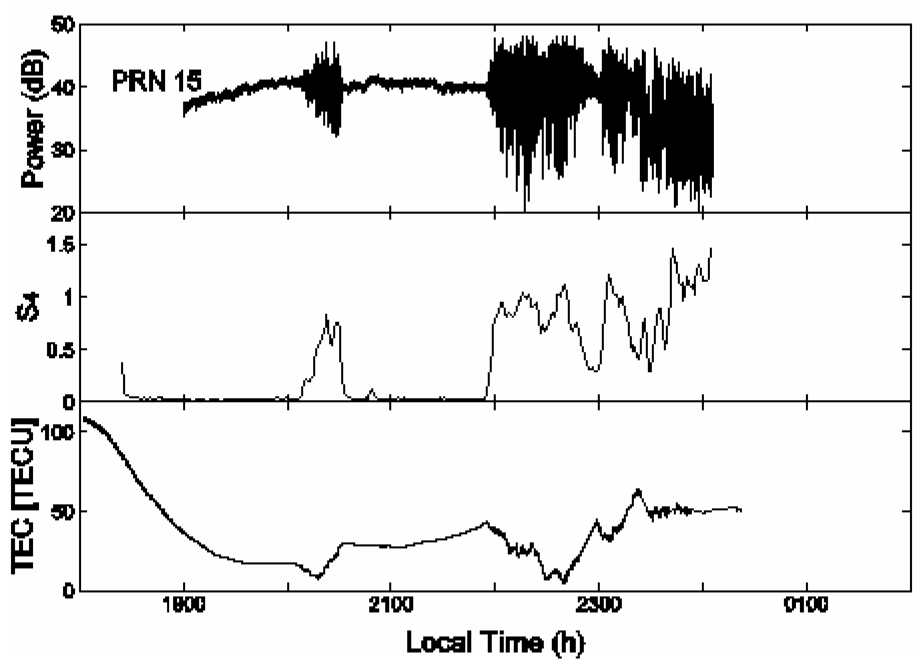


Plasma bubble can affect radio scintillation (GPS L1 frequency), S4, and TEC

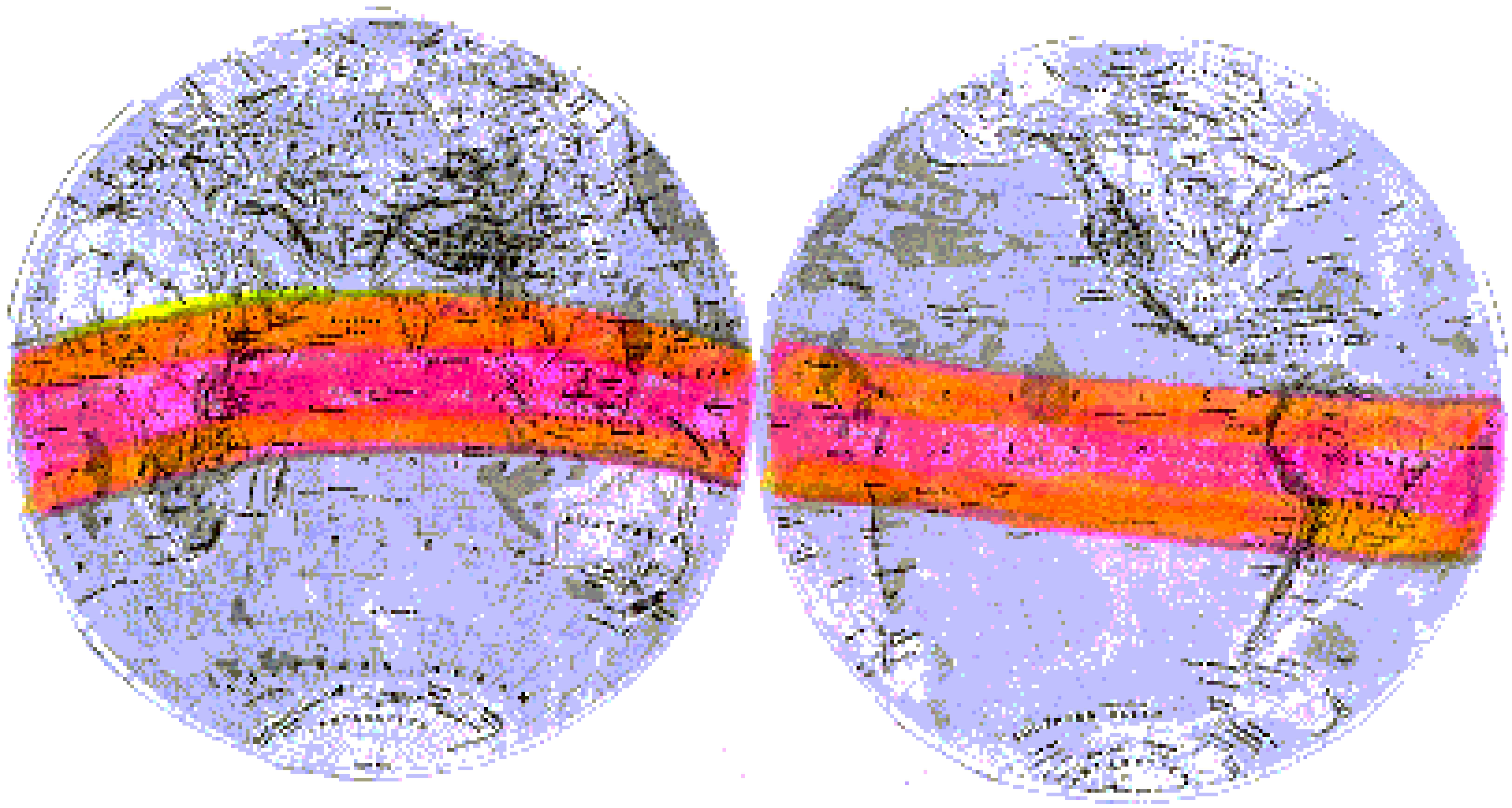

a narrow band around equator that is affected by scintillations

Note: the location of the band is determined from magnetic equator

Kennewell and McDonald [2010]

# Solar cycle variation in plasma bubble occurrence

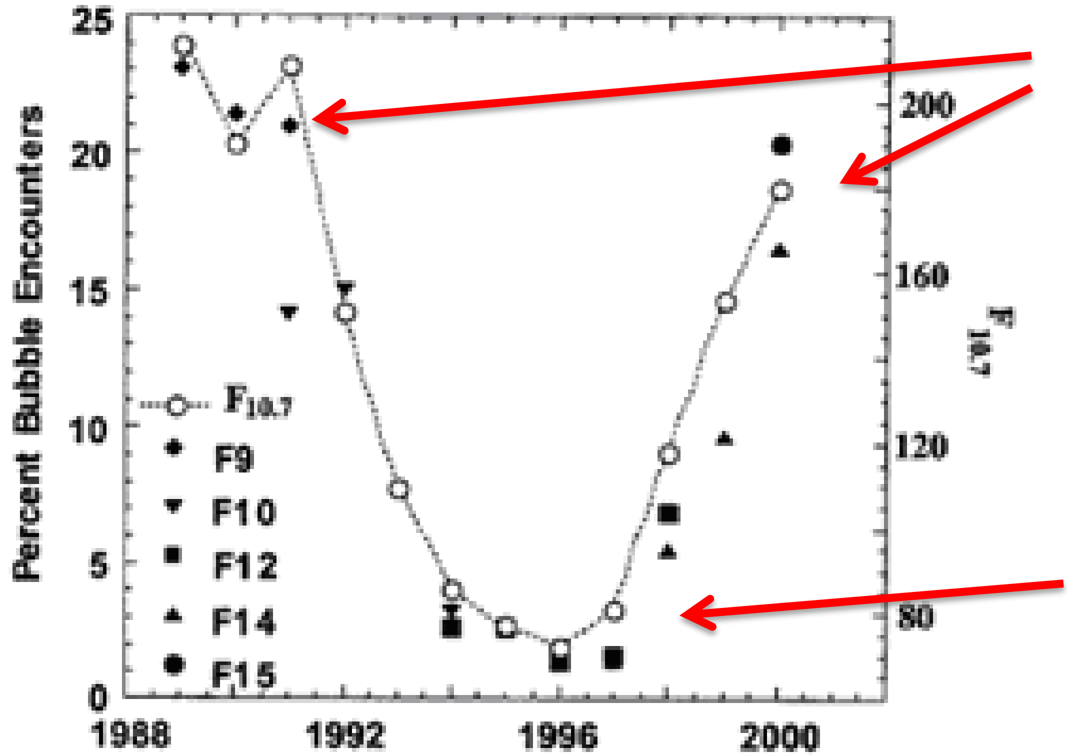


higher occurrences
near solar max

lower occurrences
near solar min

**Fig.** Solar cycle dependence of bubble occurrence rate observed by DMSP [Huang et al., 2002]

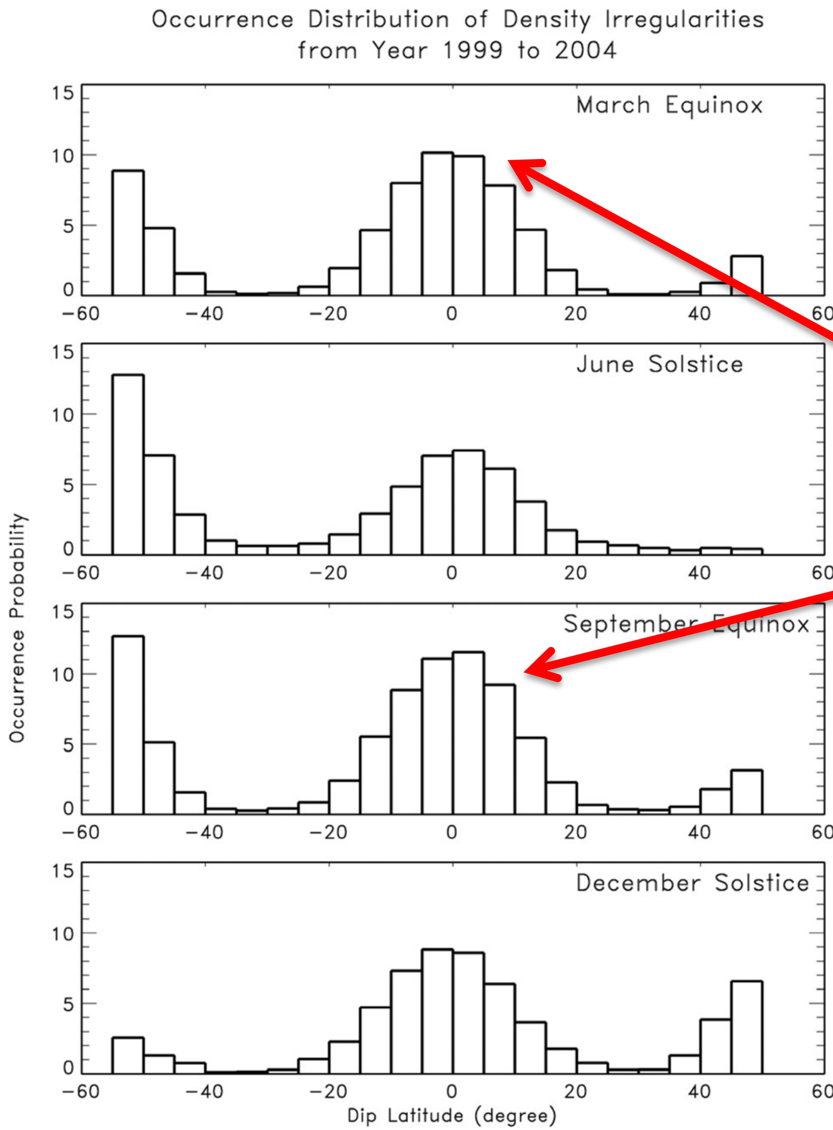


seasonal variation
in the occurrence of
plasma bubble

higher occurrences
near equinoxes

**Fig.** Latitude distribution of bubbles observed by ROCSAT-1 [Su et al., 2006].

Stening [2003]

higher S4 occurrences near equinoxes

Parepare, Indonesia

mlat = -12.6 deg

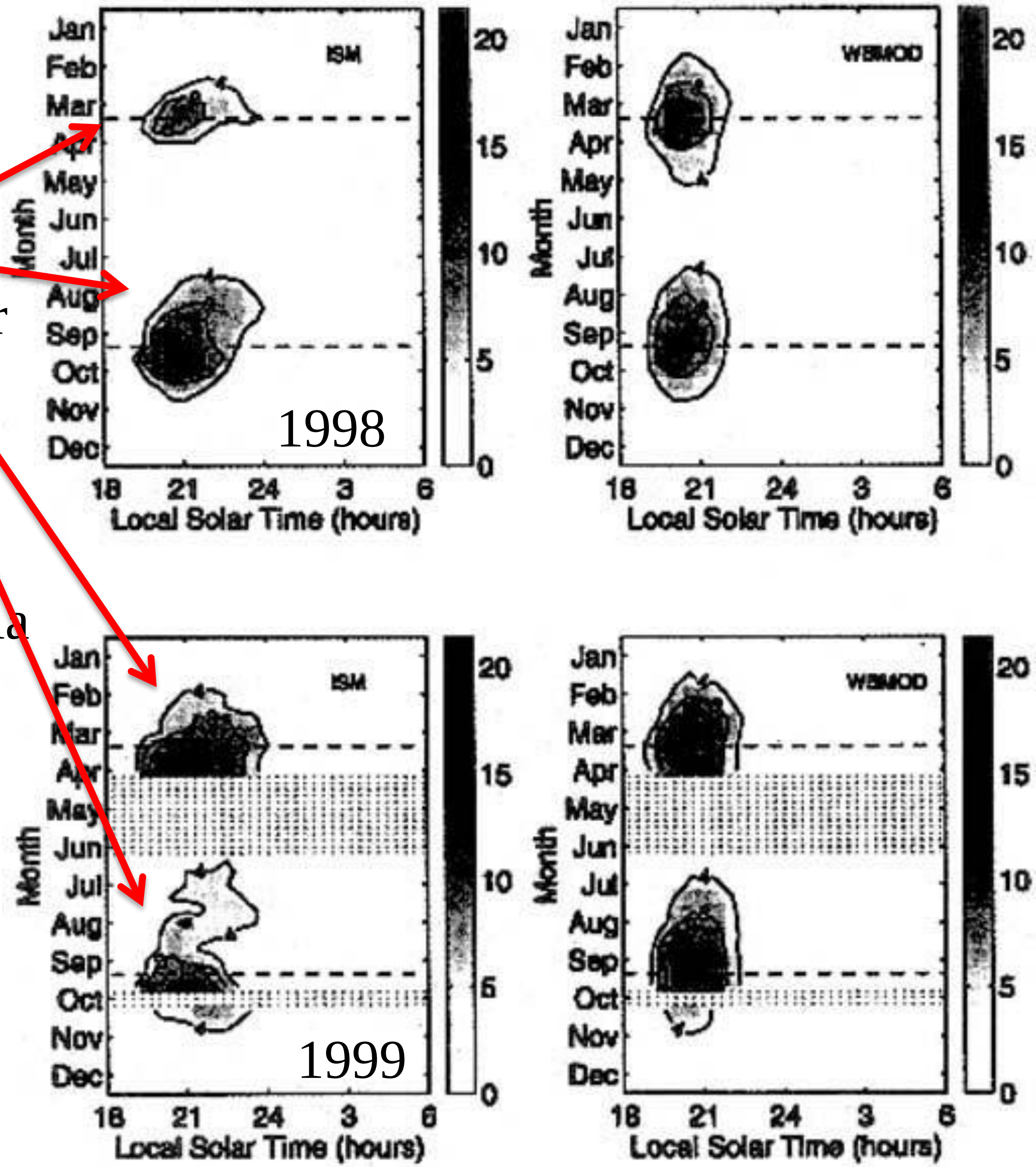

# TIMED [LEO]

## *(Thermosphere, Ionosphere, Mesosphere Energetic Dynamics)*

- Earth orbiter 625 km, measures UV to NIR spectral radiance of Thermosphere, Mesosphere, Ionosphere, 60-180 km (intercept signatures, backgrounds)
- **Launched December 2001**, 2-year mission
  - **Autonomous onboard GPS navigation <u>(no ground tracking needed)</u>**
  - **Pulse cryocooler for optics (space qualification)**
  - **UV spatial scanning spectrograph (shake down algorithms for DMSP space sensing instrument)**
  - **Doppler interferometer for wind and temperate (moving target velocity)**

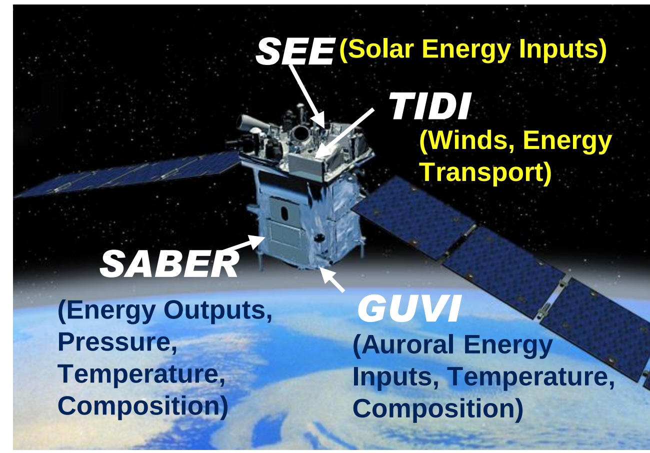


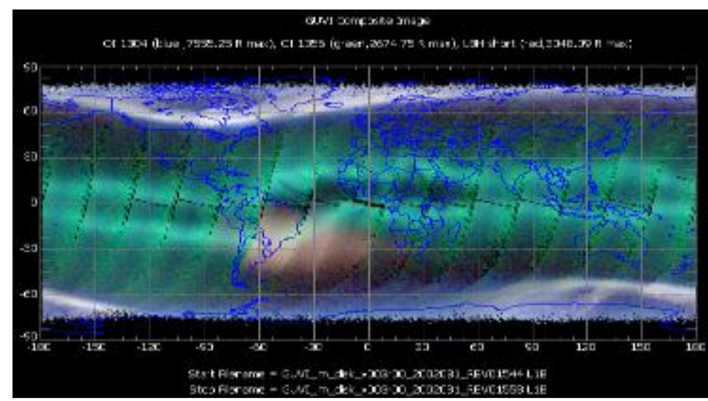

***TIMED** payloads are operated directly by scientists in a secure, authenticated manner, with autonomous deconfliction much like the vision for tactical commanders requesting space services*

# DMSP Satellite

The Defense Meteorological Satellite Program (DMSP) designs, builds, launches, and maintains satellites monitoring the meteorological, oceanographic, and solar-terrestrial physics environments.

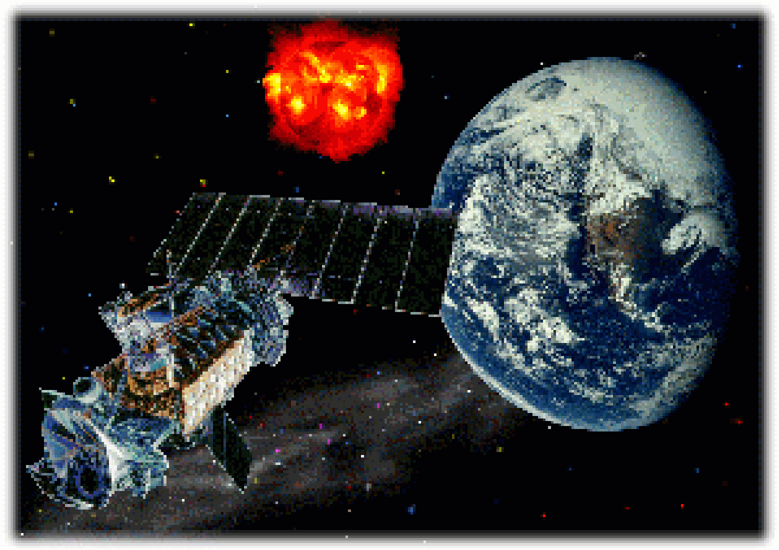

Artist's concept of the DMSP satellite

DMSP satellite:

- Nearly circular polar orbiting satellite at roughly 835 km.
- The SSJ4 instrument package detects precipitating ions and electrons from 32 eV to 30 keV [Hardy et al., 1984] (the detector looks up).
- SSUSI instrument images in UV wavelengths
- One complete 19 point ion and electron spectrum is obtained for each second, during which time the satellite moves ~7.5 km.

# FUV spectrograph imaging technique used by TIMED/GUVI and DMSP/SSUSI

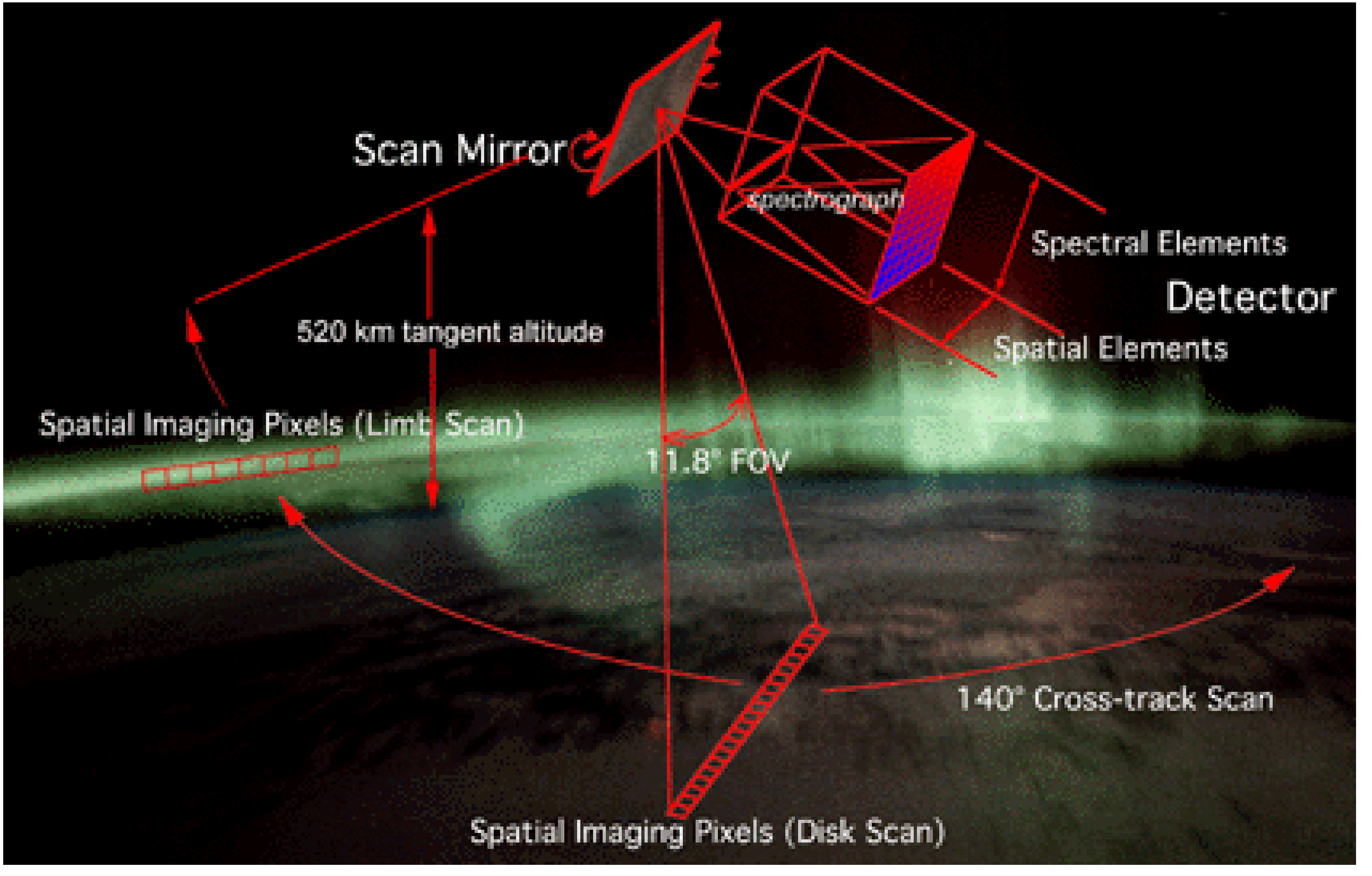

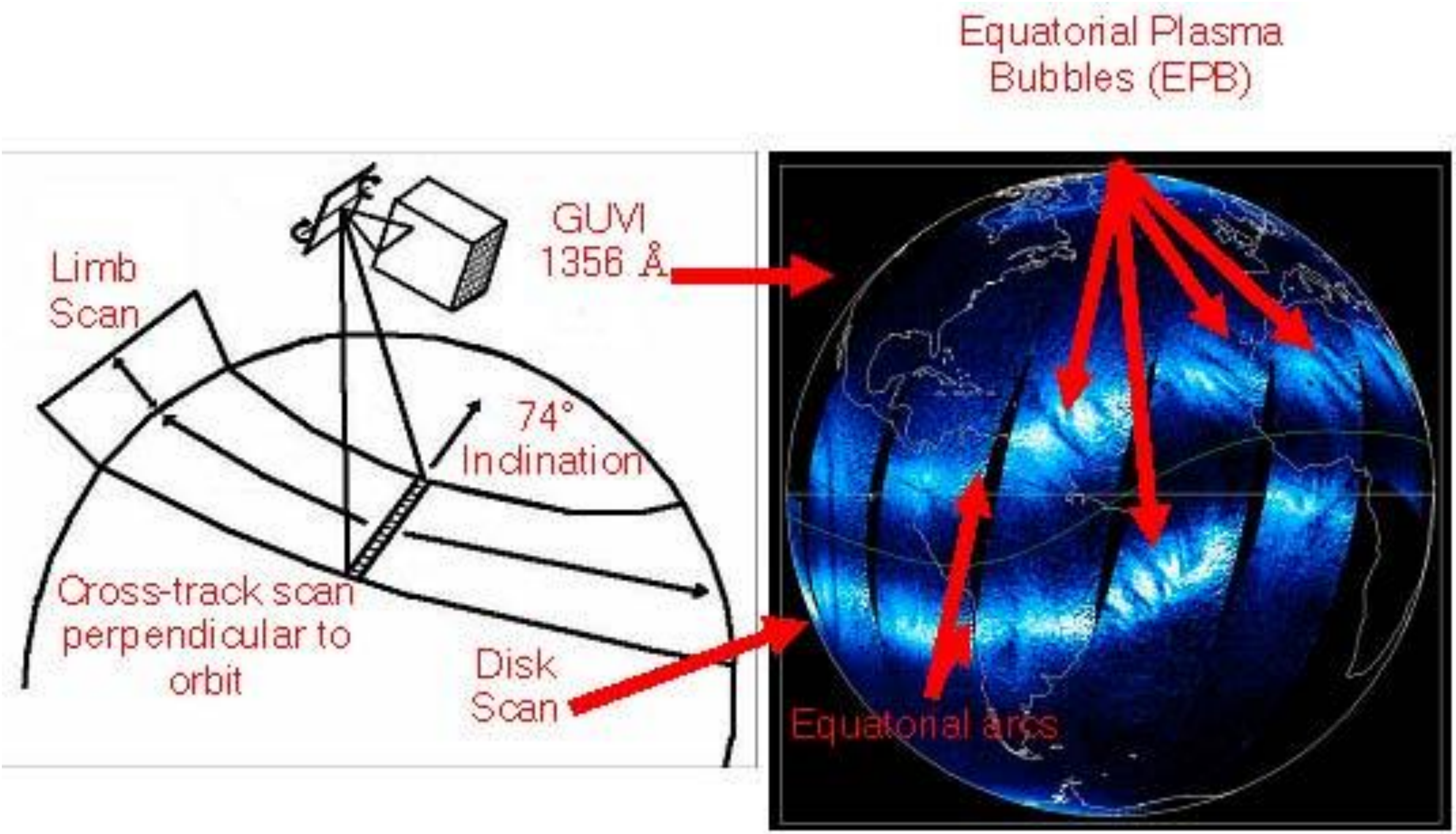
Equatorial Plasma
Bubbles (EPB)
GUVI
1356 Å
Limb
Scan
74°
Inclination
Cross-track scan
perpendicular to
orbit
Disk
Scan
Equatorial arcs

*The two distinguishing phenomena in the low-latitude F region are the equatorial ionization anomaly (EIA) and equatorial plasma bubbles (EPB).*

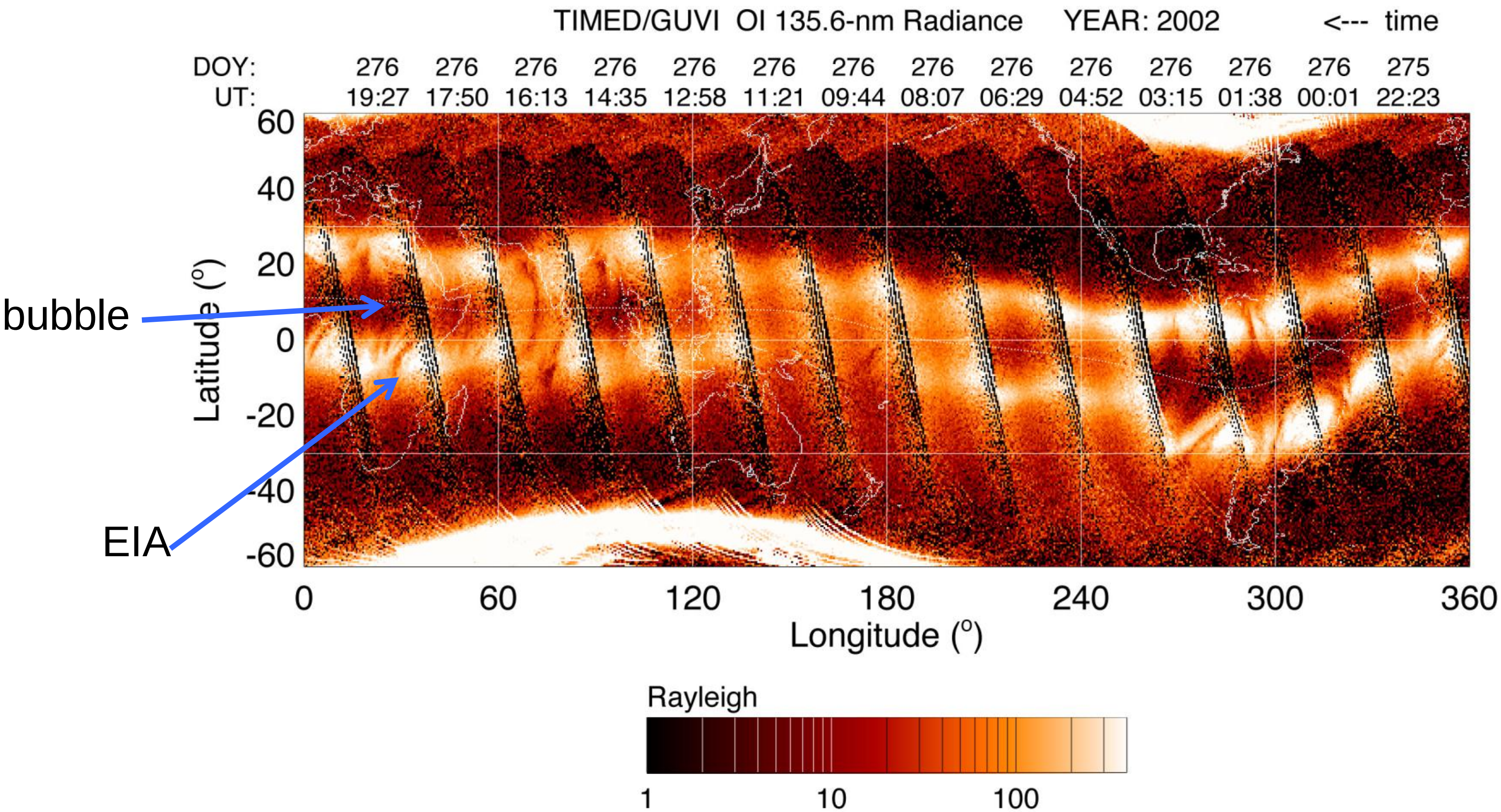


Nighttime O I 135.6-nm radiance map produced by using the TIMED/GUVI data.

$$O^+ + e \longrightarrow O^* \longrightarrow O + 135.6\text{-nm emission}$$

*Kil et al.* [2009]

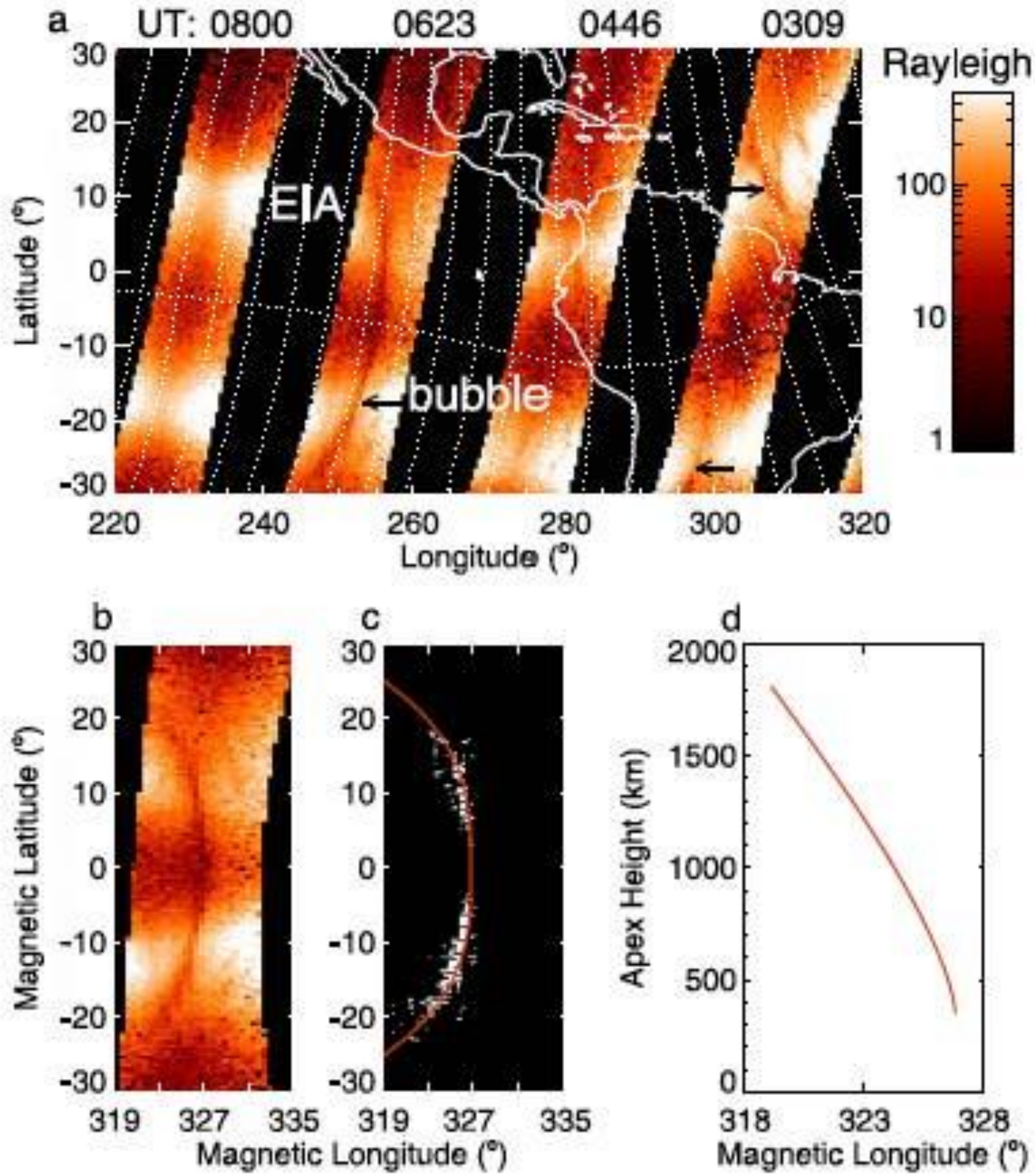

the bubble image mainly reflects the condition at peak density altitude where the contrast between depleted field line and its neighbors is the sharpest

*Kil et al.* [2009]

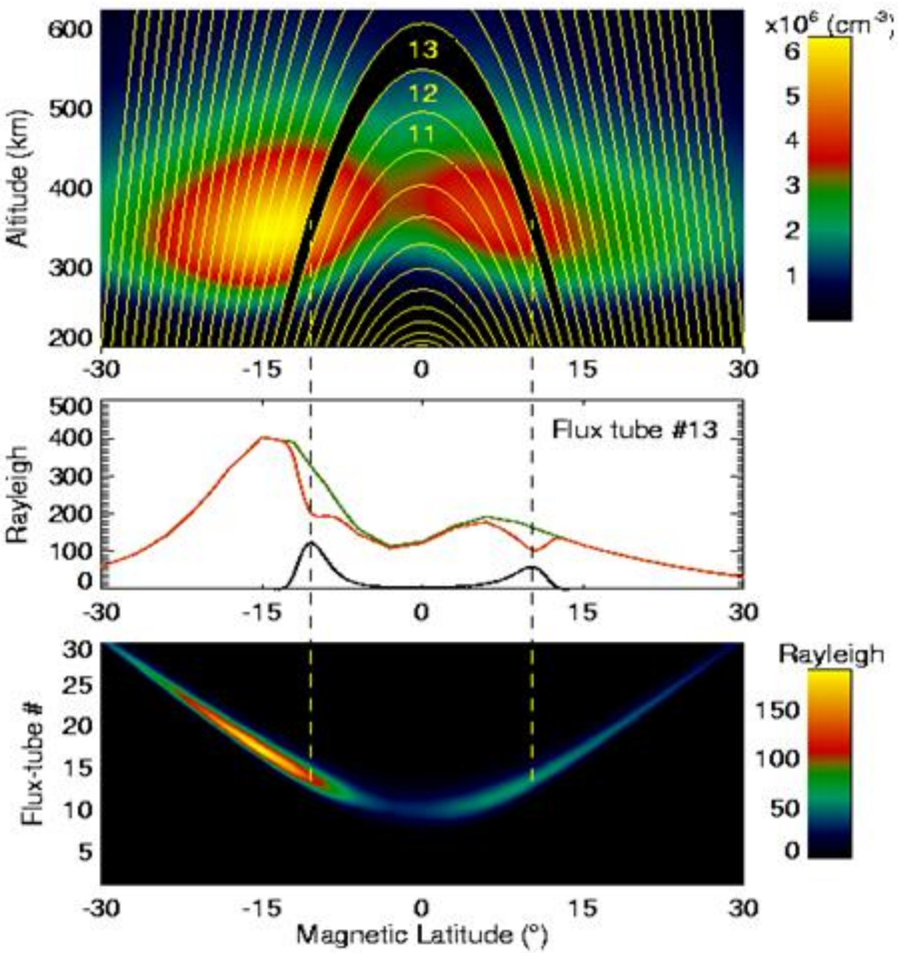


**Fig.** Test of the detection of a plasma depleted magnetic flux by optical observations.

## *Zonal shear exists in plasma drift*

mean velocity at 2000-2400 LT
near 250°E in March 2002

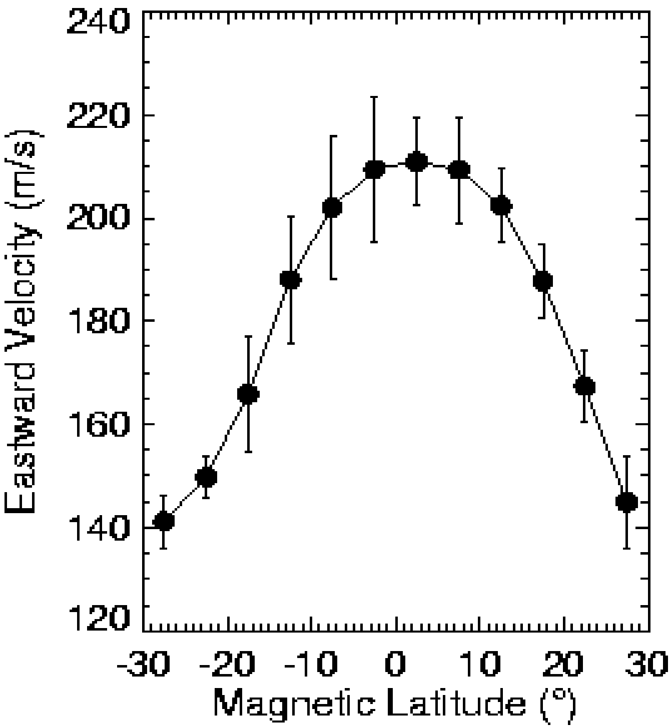


in four hours, the bubble at
the equator would travel the
farthest longitudinally

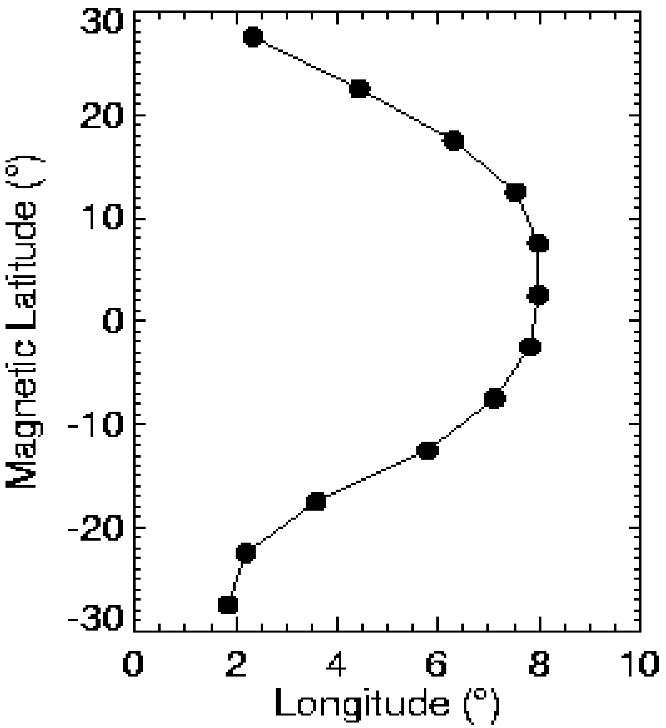


**Fig.** ROCSAT-1 observation of the zonal plasma drift at the altitude of 600 km (left) and the zonal distance traveled during 4 hours.

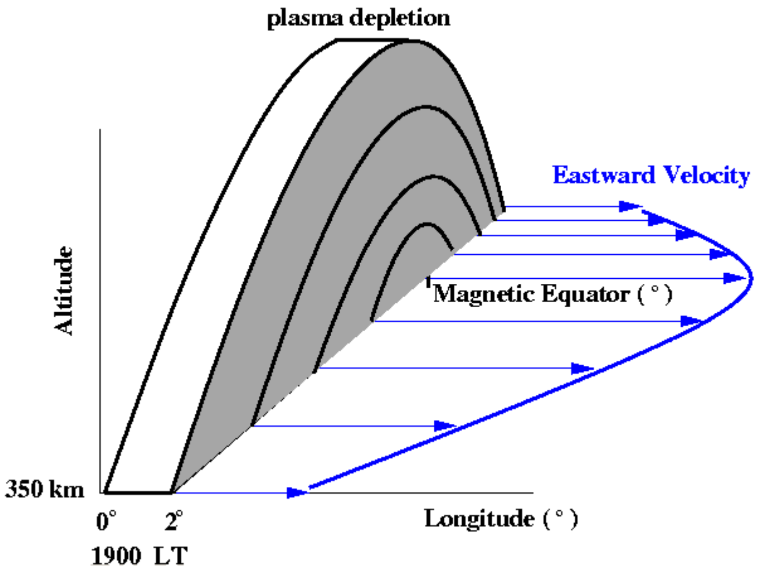

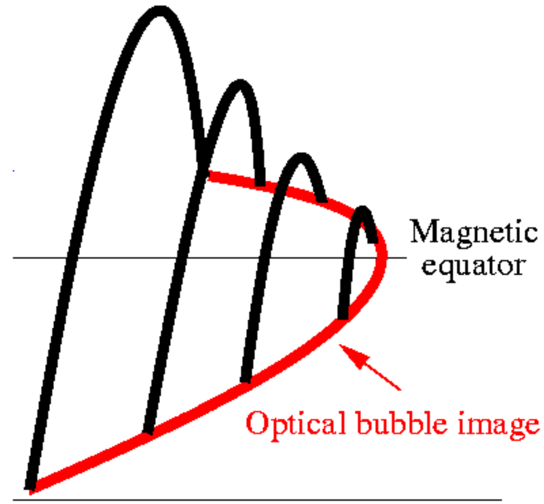

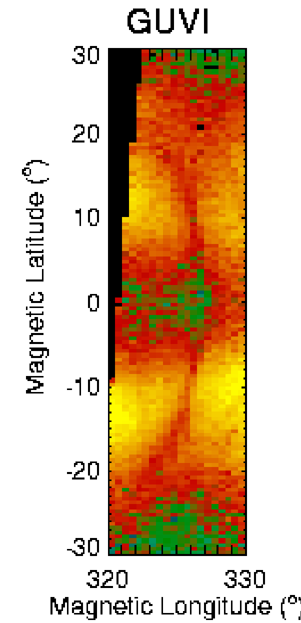


*The zonal shear flow of the ionosphere creates a "**plasma depletion shell**".*

*The intersection of the plasma depletion shell with horizontal plane at F-peak altitude creates a **backward C-shaped** optical bubble image.*

*Kil et al.* [2009]

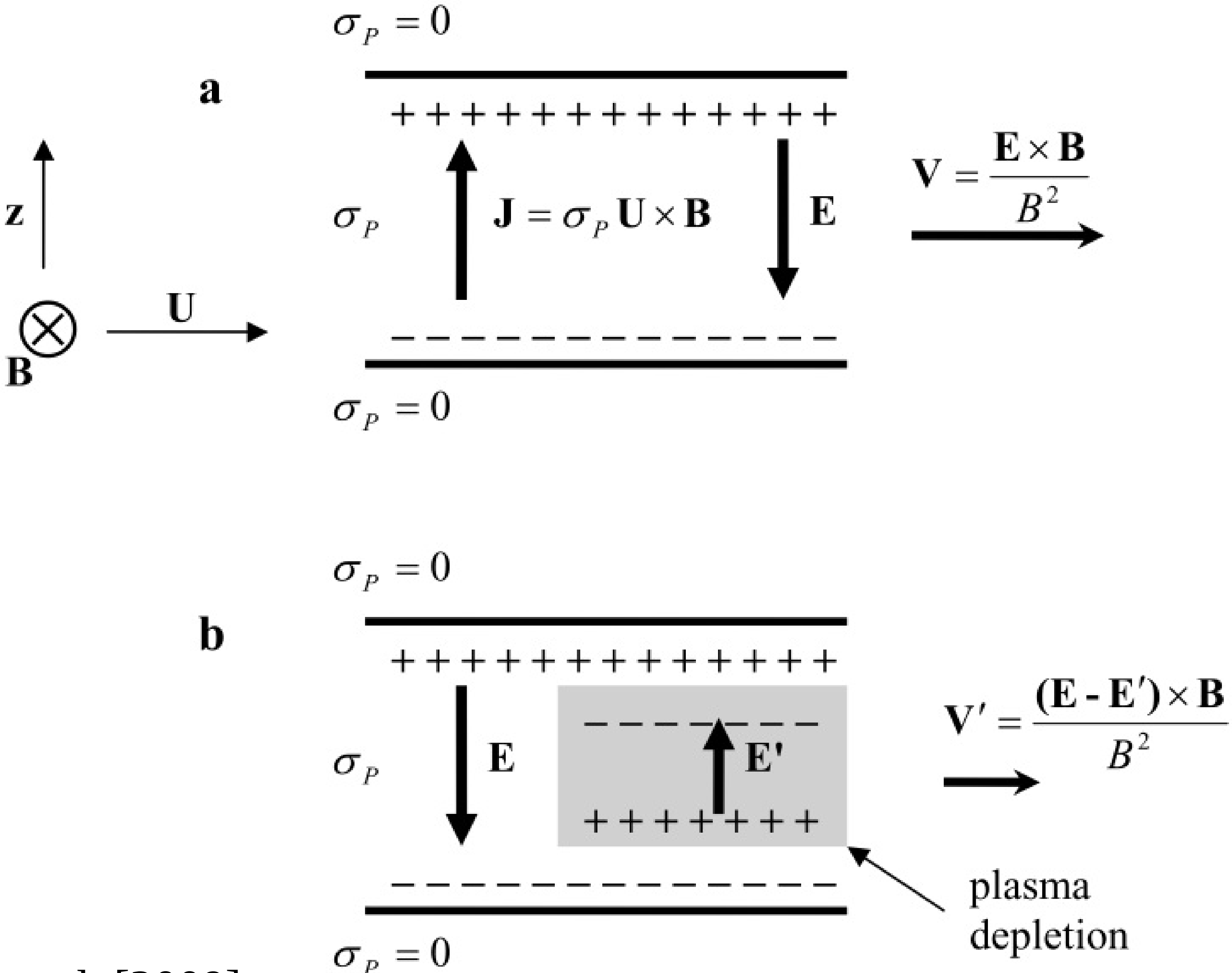


Kil et al. [2009]

# Formation of a plasma depletion shell

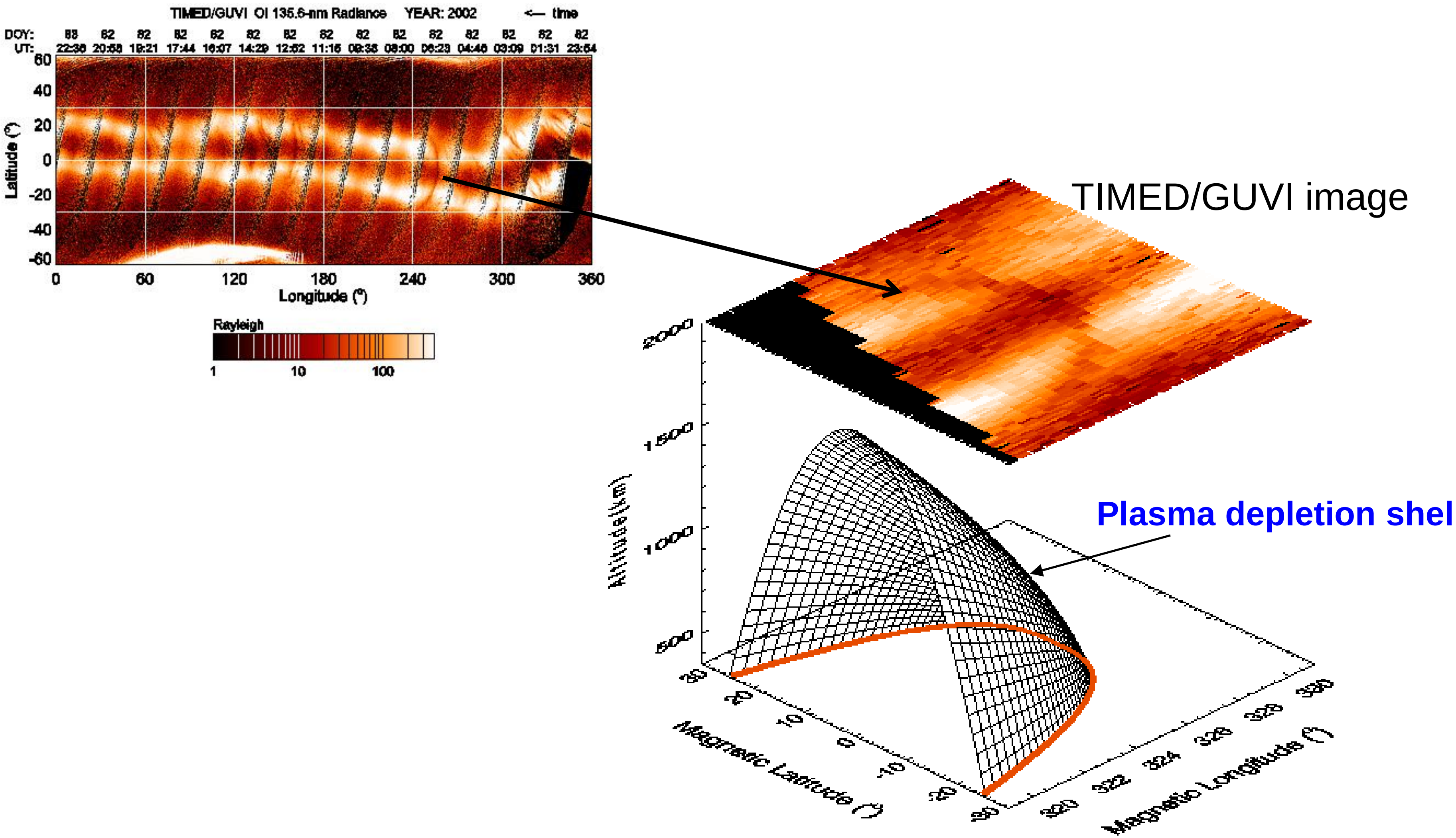


*Kil et al.* [2009]

# Plasma Bubble Detection

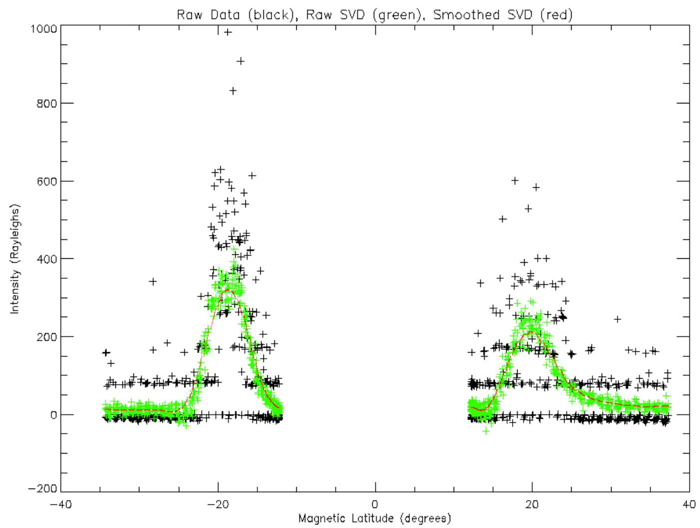


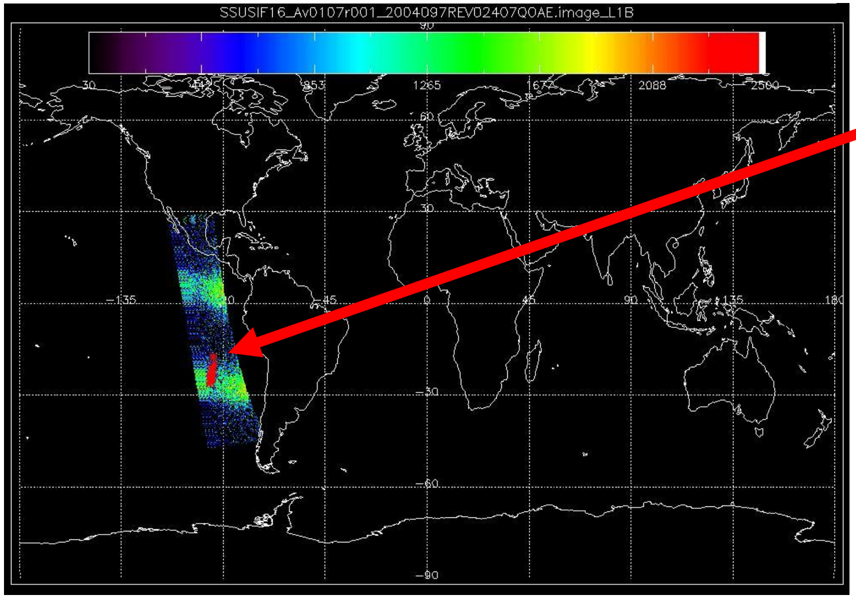


- Bubble detection algorithm currently being adapted for use with SSUSI data
- Algorithm can locate and characterize EIA peaks
- Pixels containing plasma bubbles are identified

Comberiate and Paxton [2010]

# SSUSI Observation Model

- Use tomography technique to obtain 3D images
- Assume invariance along field lines for that segment
- Distinct overlapping scans with respect to altitude vs. longitude profile allow for tomography

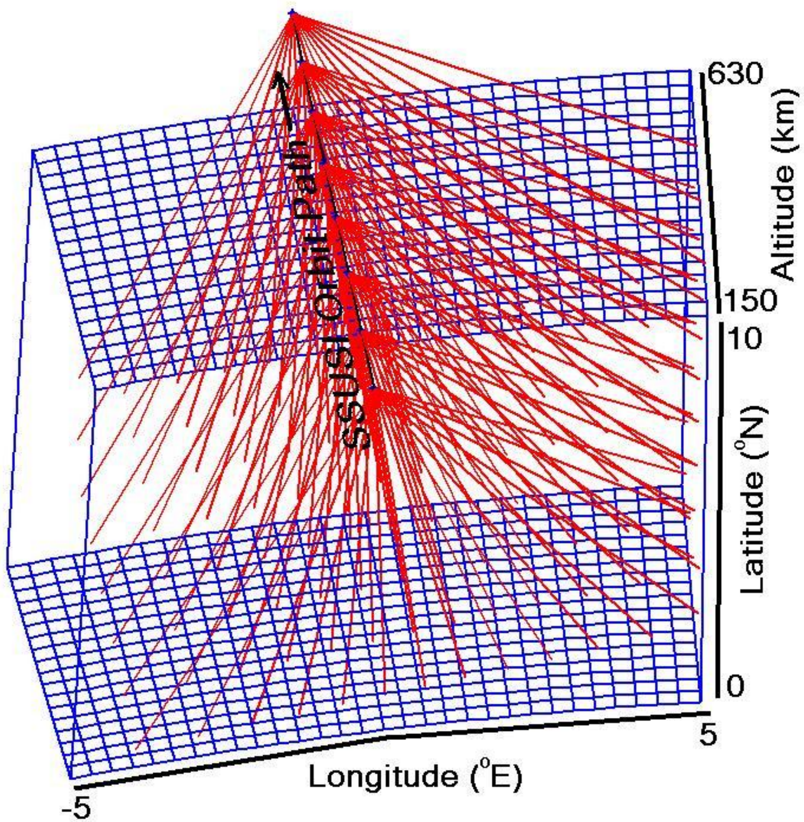


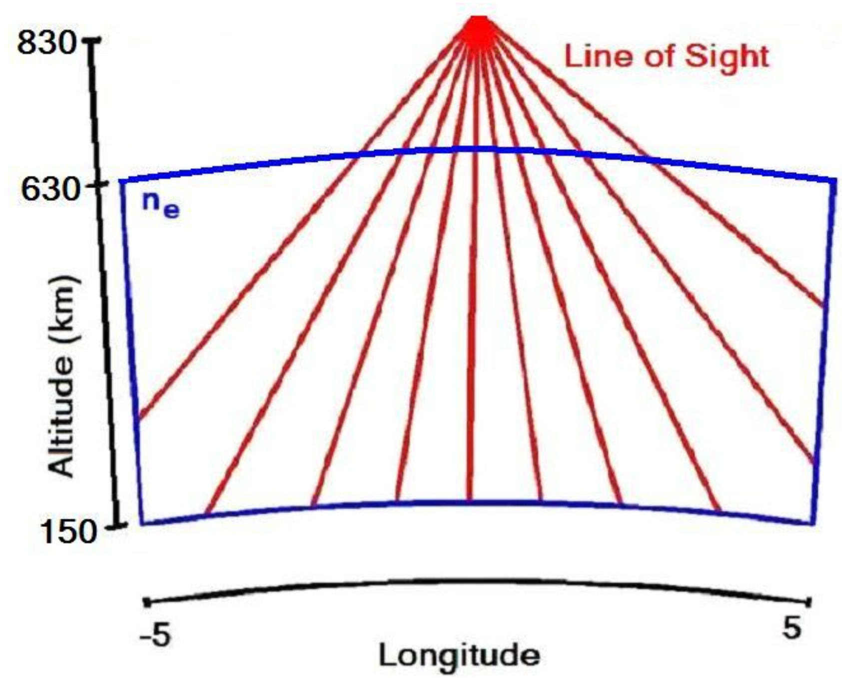

# 3-D Bubble Imaging Technique

- Tomographic inversion performed for each altitude vs. longitude slice

- 12 slices (5° latitude resolution) combined to form 3D profile

- Main sources of error include low SNR for counting statistics, limited latitudinal resolution, and limited-angle viewing geometry

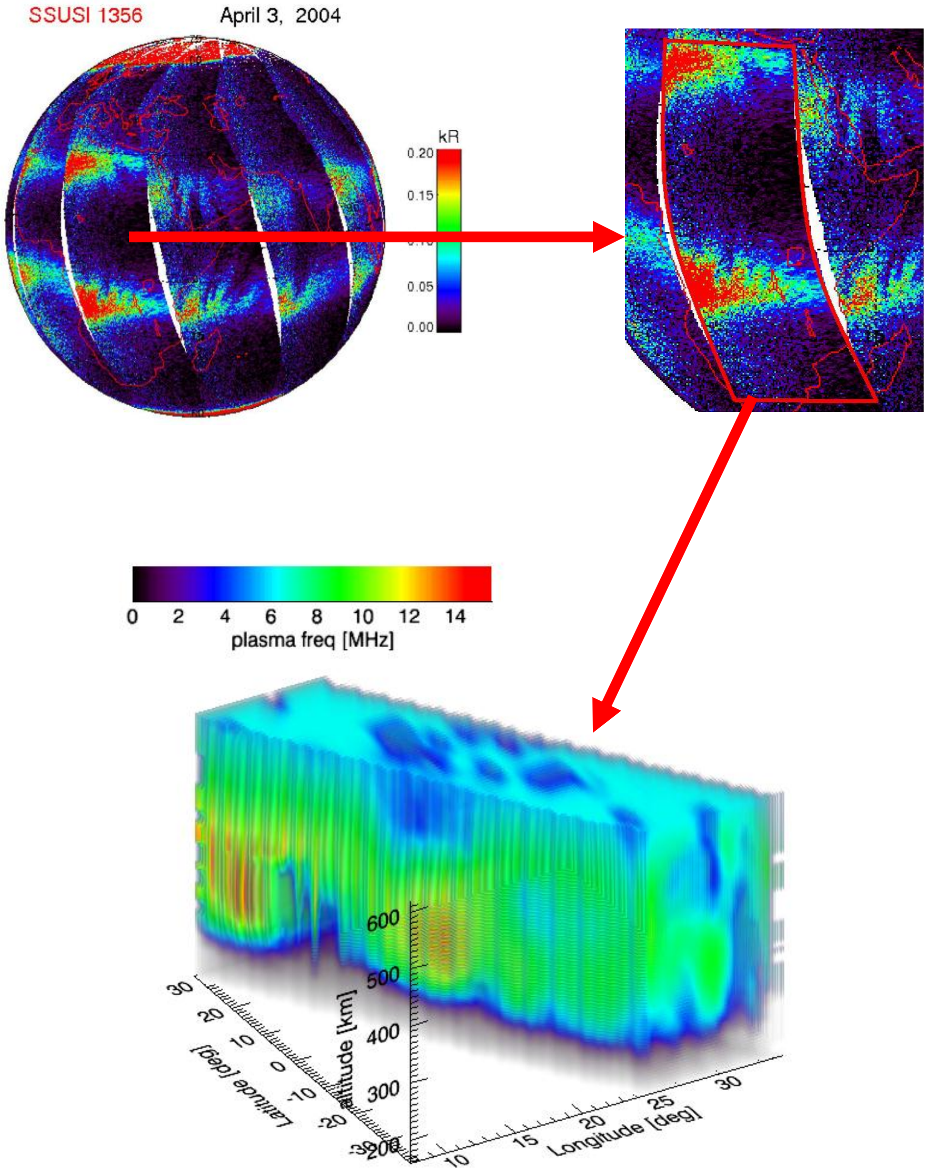

# SSUSI Bubble Imaging

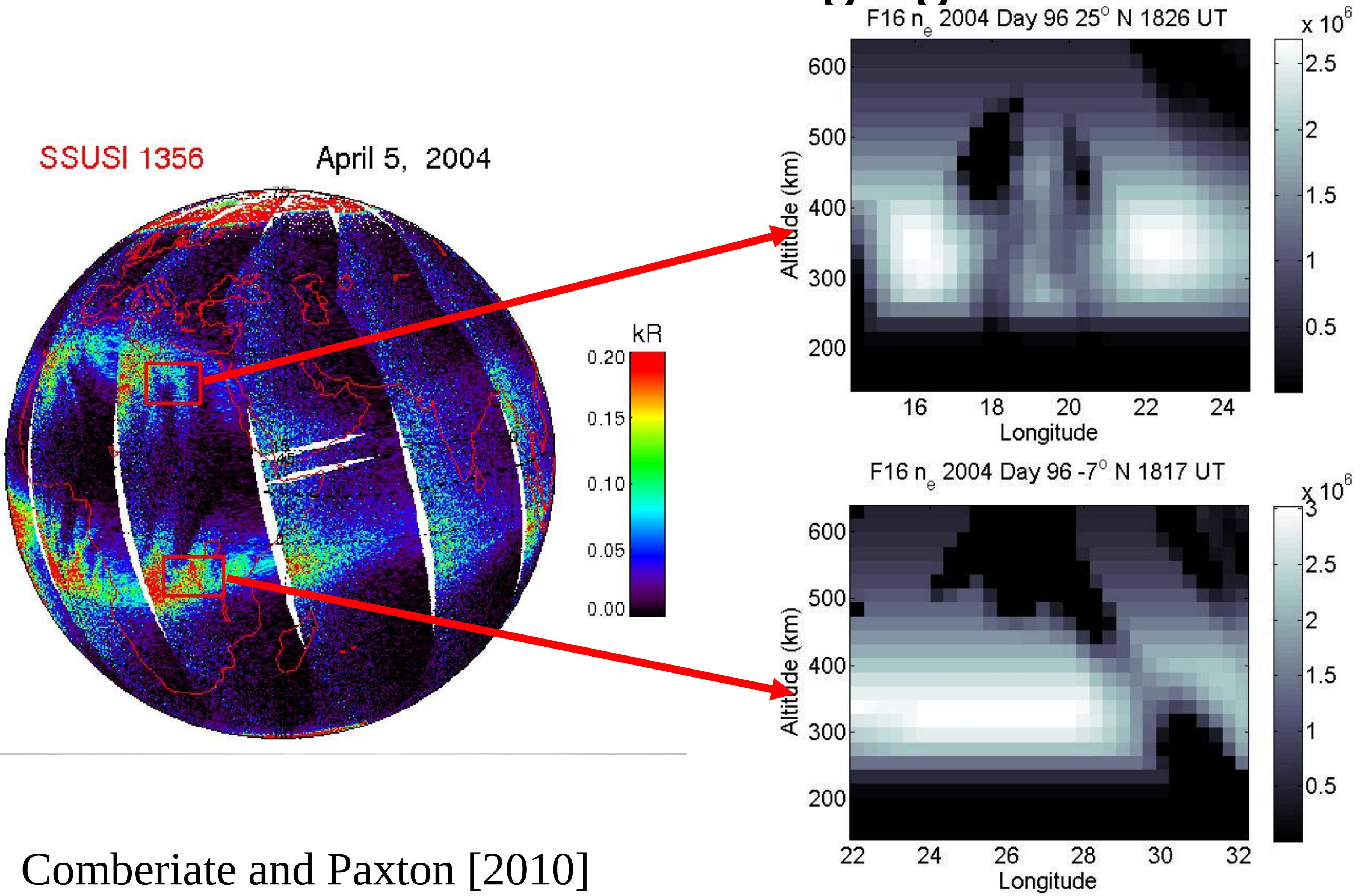


Comberiate and Paxton [2010]

# Bubble Formation

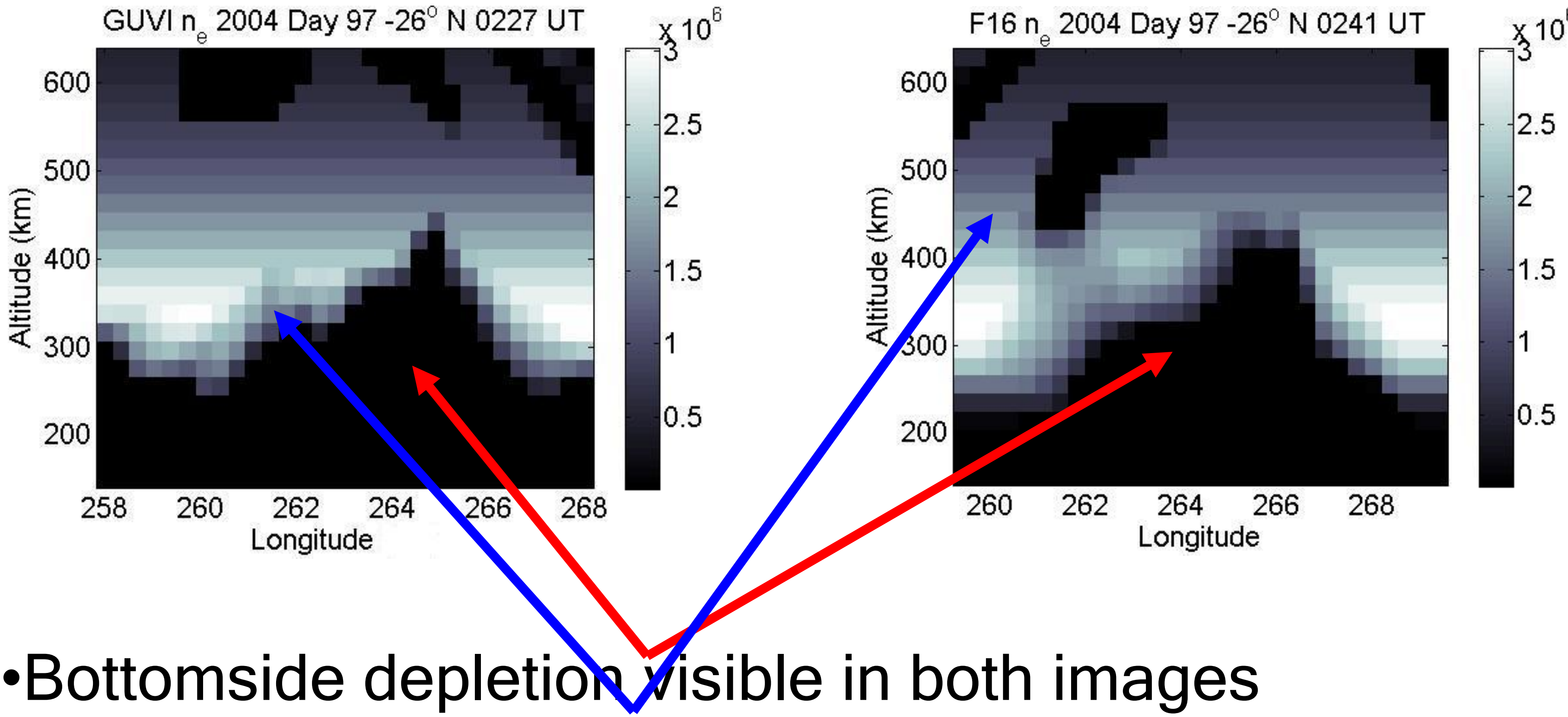


- Bottomside depletion visible in both images
- Plume growth (15 min between images)
- Depleted region drifts East at approx. 100 m/s

TIMED GUVI and DMSP SSUSI have broken new grounds in plasma bubble studies

Comberiate and Paxton [2010]

# 3. Space weather forecasting with machine learning

The underlying physics of many space objects and phenomena is often complex and not well understood, but progress can be achieved through the use of advanced or even standard machine learning and artificial intelligence principles

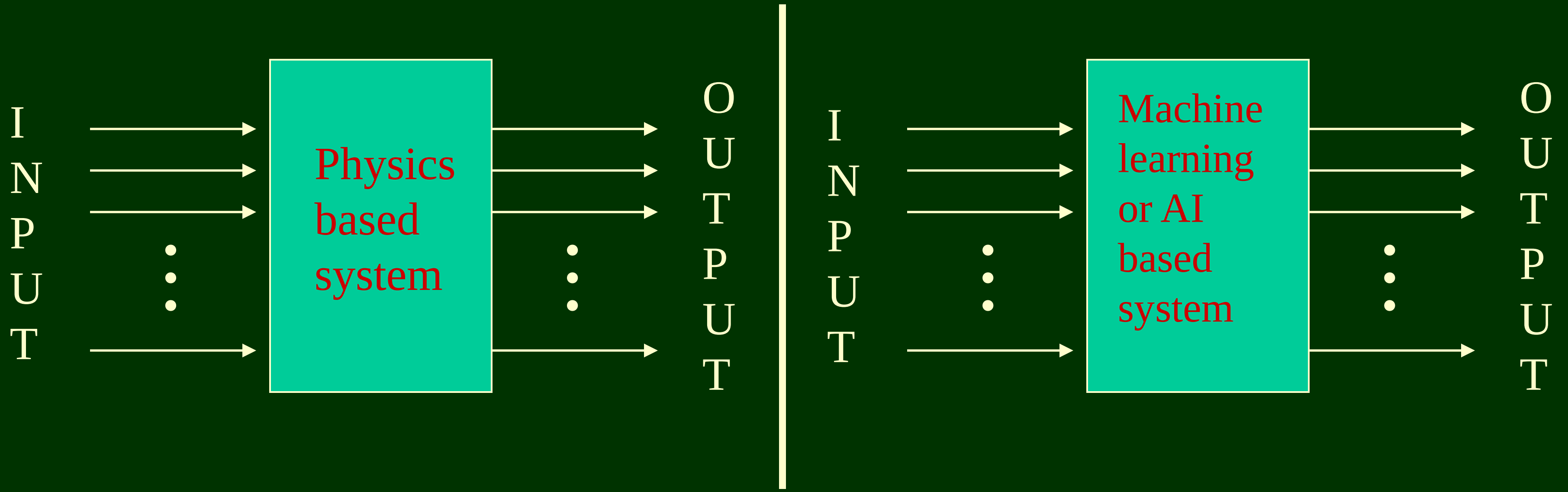

# Neural Network

- A NN architecture with 1 hidden layer [a class of multi-layer feedforward network (MLFN)]

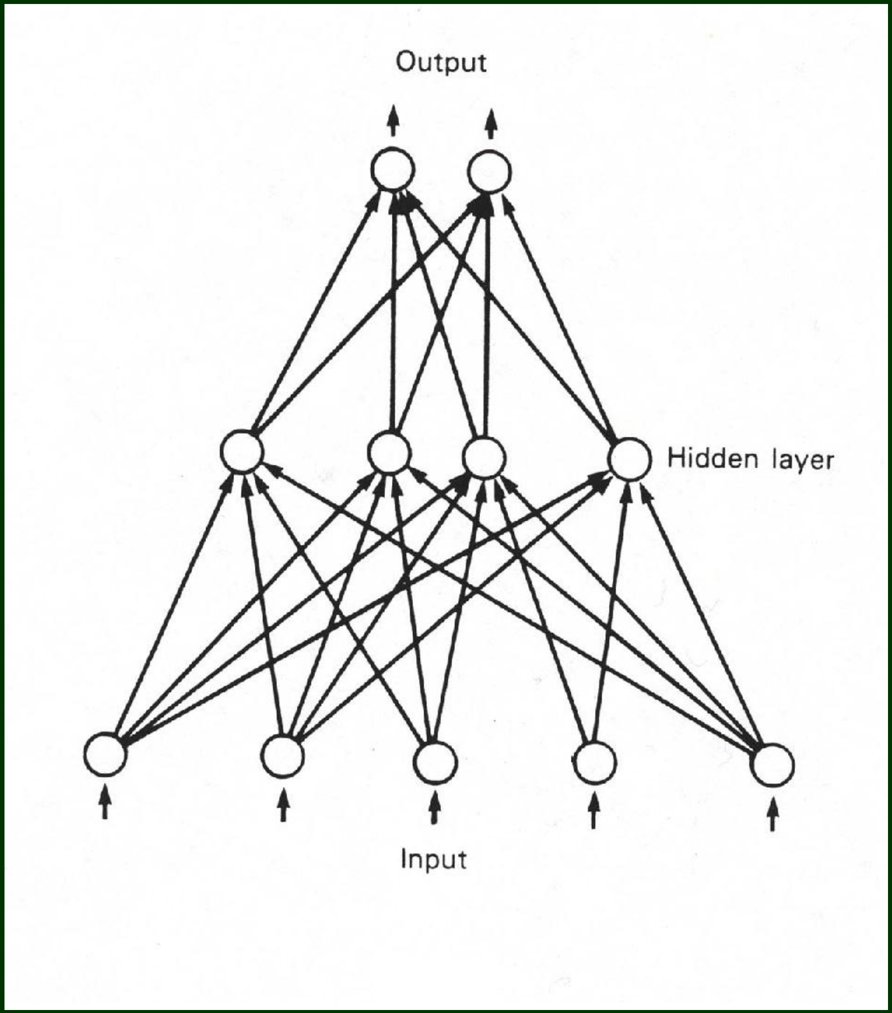


The intelligence lies in the connections between the nodes

A class of NN with 0 hidden layer is called perceptron

# Two applications of neural networks

a. Kp forecast models
b. HF backscatters from ionospheric irregularities (clutters)

# 3.a Kp forecast models

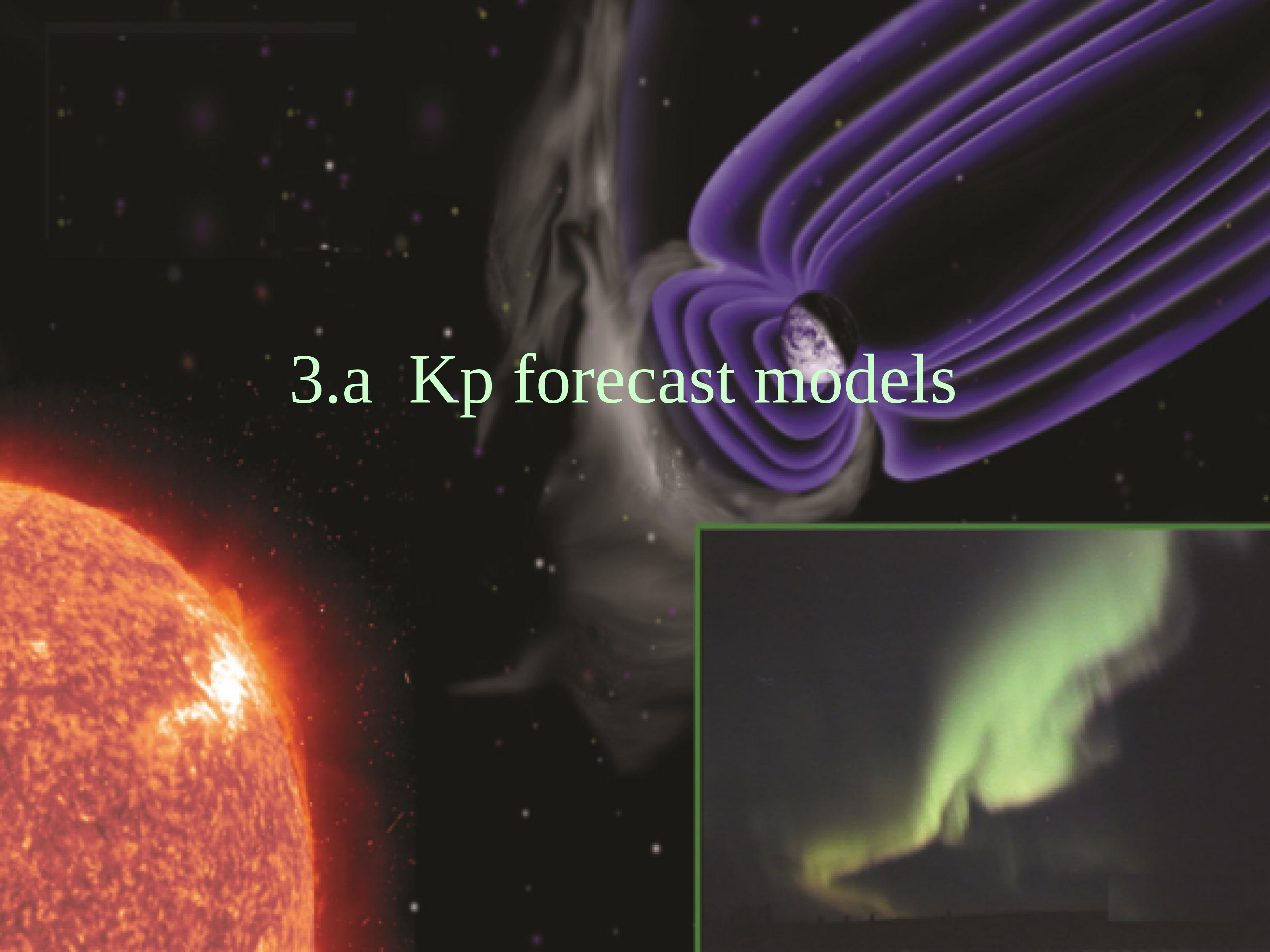

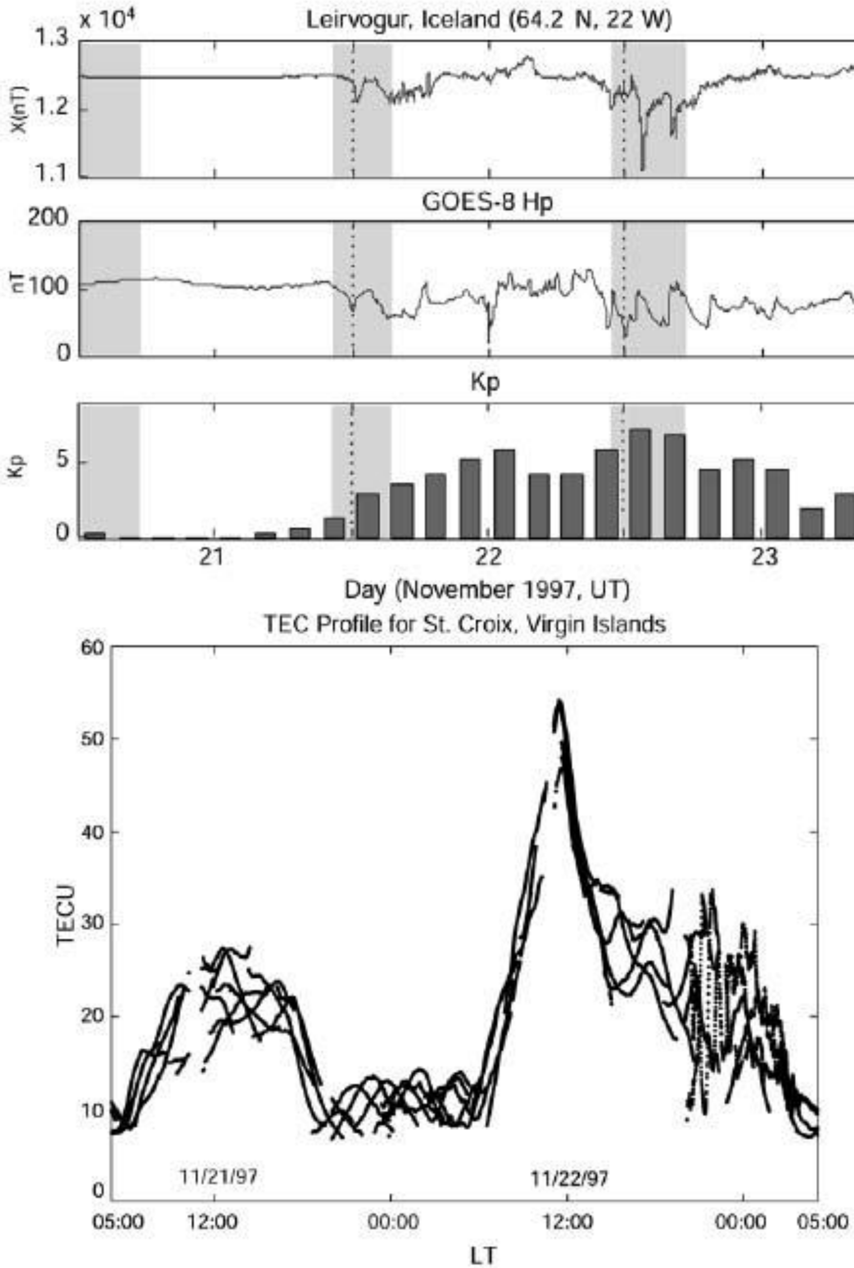


**Figure 1.** The top three panels show, respectively, the pole-ward component of the magnetic field, measured at Leirvogur, Iceland (top); data from the fluxgate magnetometer on the geostationary satellite GOES-8, which is located at 75° W longitude (middle); Kp indices for the same period. The bottom panel shows the total equivalent vertical electron content (1 TECU = $10^{16}$ $m^{-2}$) for all GPS satellites in view from St. Croix near Puerto Rico on November 21-22, 1997; LT = UT – 4 hours [after *Kelley et al.*, *2000*].

Bhattacharyya and Basu [2002]

- Kp is a geomagnetic activity index
- During storm, Kp is high
- TEC near noon is twice as large as the previous day

geographic lat = 18 deg N

# Pandey and Dashora [2005]

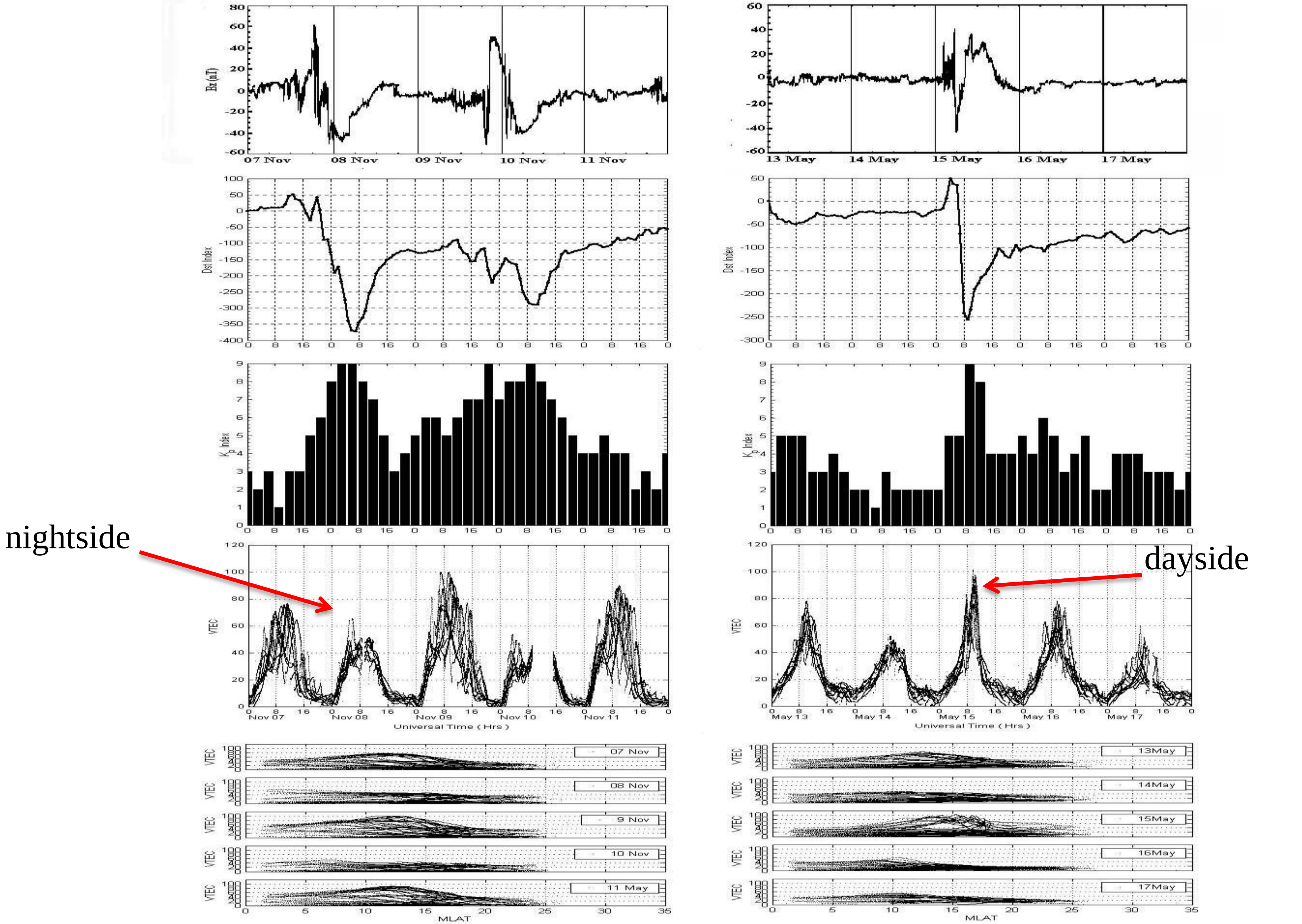


Udaipur (mlat = 15.3 deg) near EIA

# Background and Motivations for developing Kp forecast models

- Moderate and high activities are notoriously difficult to predict [Joselyn, 1995].
- Real-time magnetometer data can be used to calculate nowcast Kps, which could improve the accuracy of the forecast Kps.

Why Kp?

- Kp is one of the most popular global indices.
- Kp has been playing significant roles in space weather, e.g., satellite drags, satellite communication, etc.
- Many magnetospheric and ionospheric models require Kp as an input parameter, e.g., T89 magnetic field model, Fok ring current-radiation belt model, MSFM, OVATION, etc.
- The long uninterrupted Kp record since 1932 makes it ideal for studying solar-wind magnetosphere interactions, e.g., the solar cycle effects, etc.

# The APL Kp forecast models

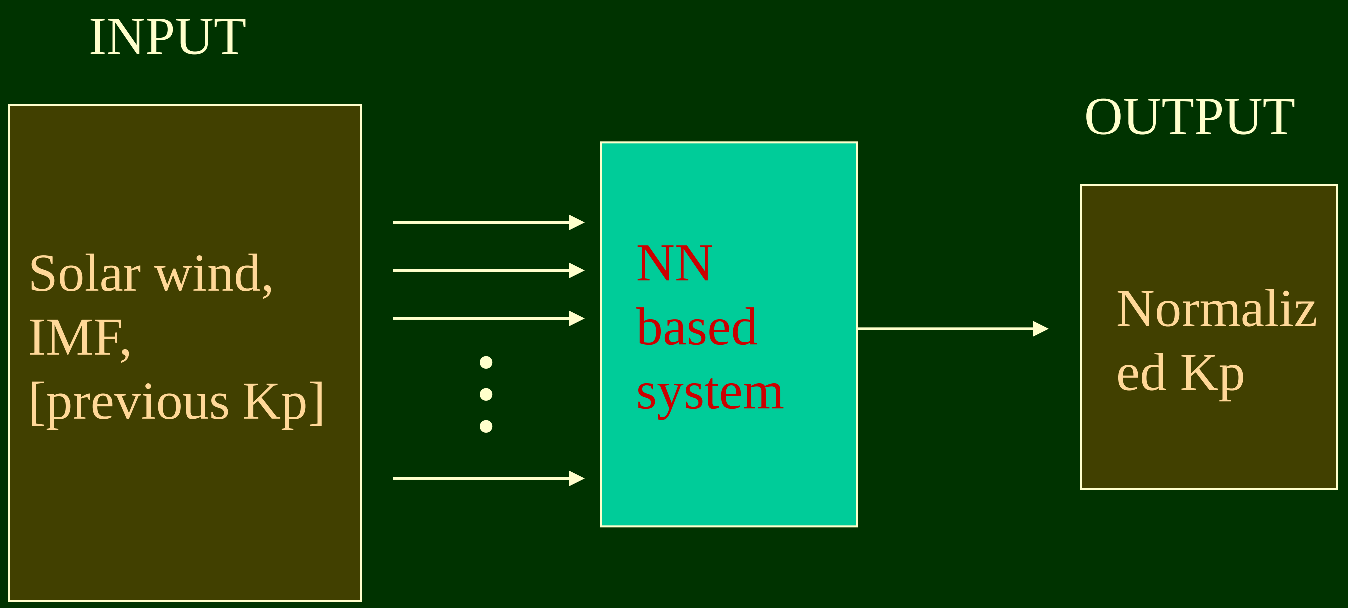

# Summary and Conclusion

- In order to satisfy different needs and operational constraints, we developed 3 Kp forecast models:
  1. APL model 1
     - Input: ACE solar wind n, Vx, IMF |B|, Bz, and nowcast Kp
     - Output: ~1-hr ahead Kp forecast
  2. APL model 2
     - Input: same as model 1
     - Output: ~4-hr ahead Kp forecast
  3. APL model 3
     - Input: ACE solar wind n, Vx, IMF |B|, and Bz
     - Output: ~1-hr ahead Kp forecast

- Note: a very accurate nowcast Kp algorithm [Takahashi et al., 2001] can be used as an input to APL models 1 and 2.

# Summary and Conclusion

Operational at NOAA/AF

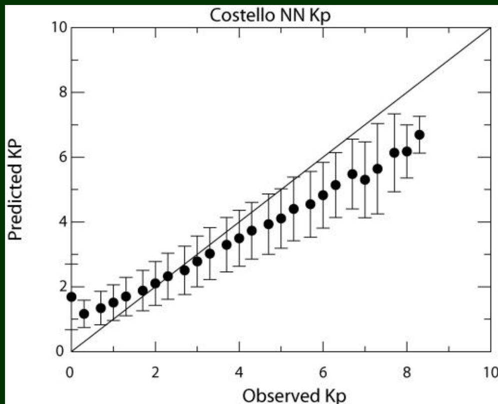


Univ. of Sheffield

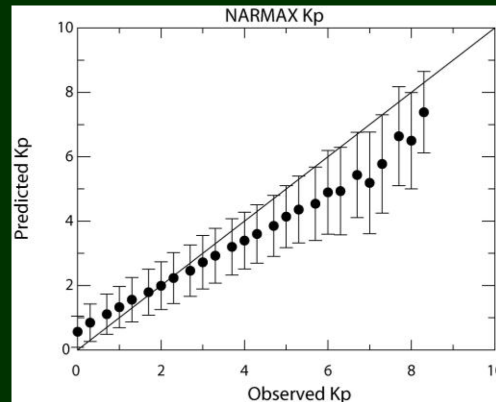


Boberg et al. [2000]
Operational at Lund Obs.

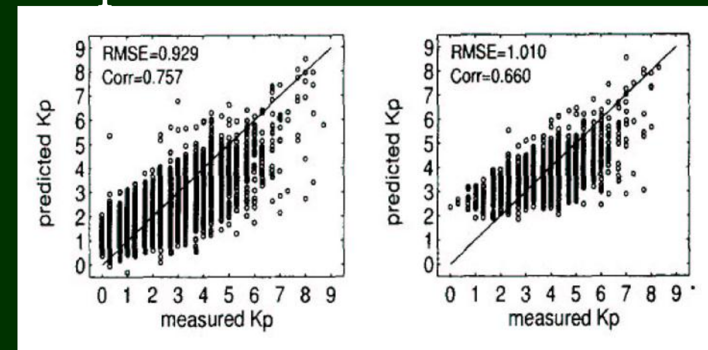


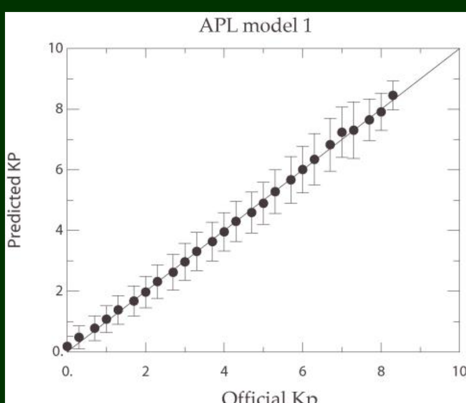


APL model 1

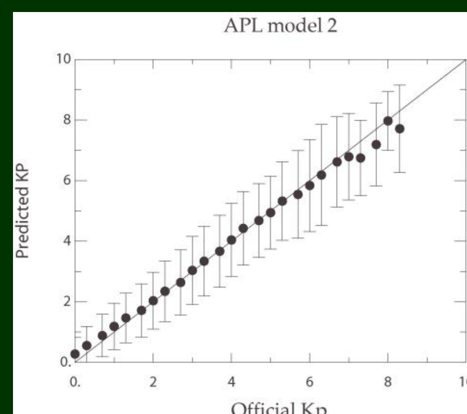


APL model 2
(4 hr ahead
forecast)

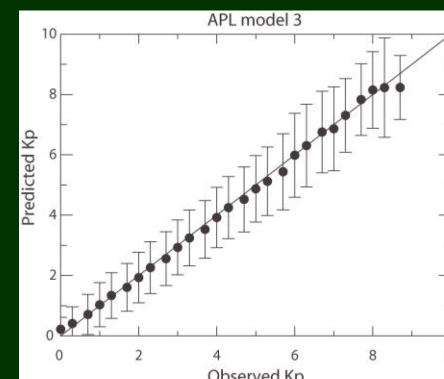


APL model 3
(purely
driven by
solar wind)

Wing et al. [2005]

# Predictive Model Performance

The skill scores are defined below (Detman and Joselyn, 1999).

The figures show the skill scores for Costello Neural Network (NN) model over 2 solar cycle periods. They show that the model performance has a solar cycle variation. The model performs better near solarmax than solarmin for active times (Kp > 3). The input parameters to the model are: solar wind V, IMF |B|, IMF Bz, and the previous Kp predictions of the model.

The skill scores are defined below (Detman and Joselyn, 1999).

Forecast

| Observed | | Y | N |
|---|---|---|---|
| | Y | x | y |
| | N | w | z |

True Skill Statistics (TSS):

$$TSS = \frac{xw - yz}{(x+y)(z+w)}$$

Gilbert Skill (GS):

$$GS = \frac{x - Ch}{((x - Ch) + y + z)}$$

GS ignores w ("correct rejection").
Ch = chance hits = (probability of Y events to occur) X (number of Y events forecasted)

$$Ch = \frac{(x+y)}{(x+y+z+w)}(x+z)$$

For TSS and GS:
Perfect forcecast = 1
Random forecast = 0

# Summary and Conclusion

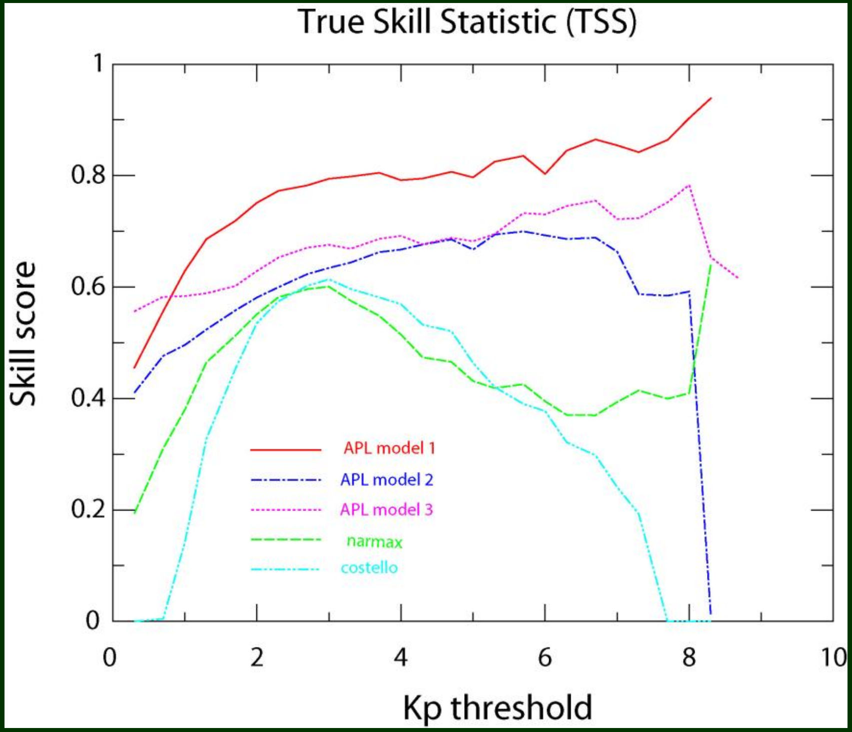


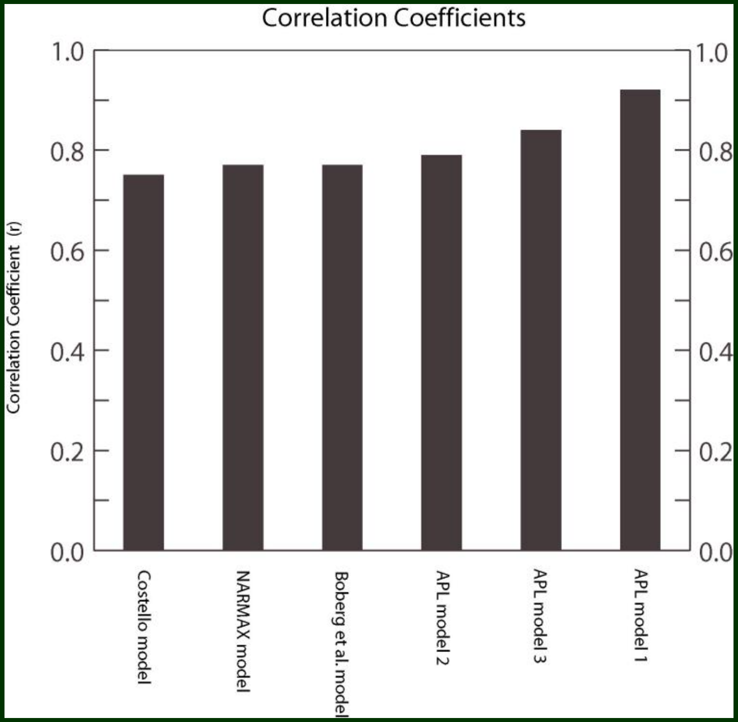


True Skill Statistic (TSS) [Detman and Joselyn, 1999] based on data spanning over 2 solar cycles.

Note: for comparisons with other published results, r is calculated over all Kp ranges and therefore, this figure <u>understates</u> the dramatic improvements the APL Kp models obtain for active times, Kp > 4.

Wing et al. [2005]

# NOAA / Space Weather Prediction Center

**Predicted Geomagnetic Activity Index using Wing Kp Model -- 12-hour Plot**

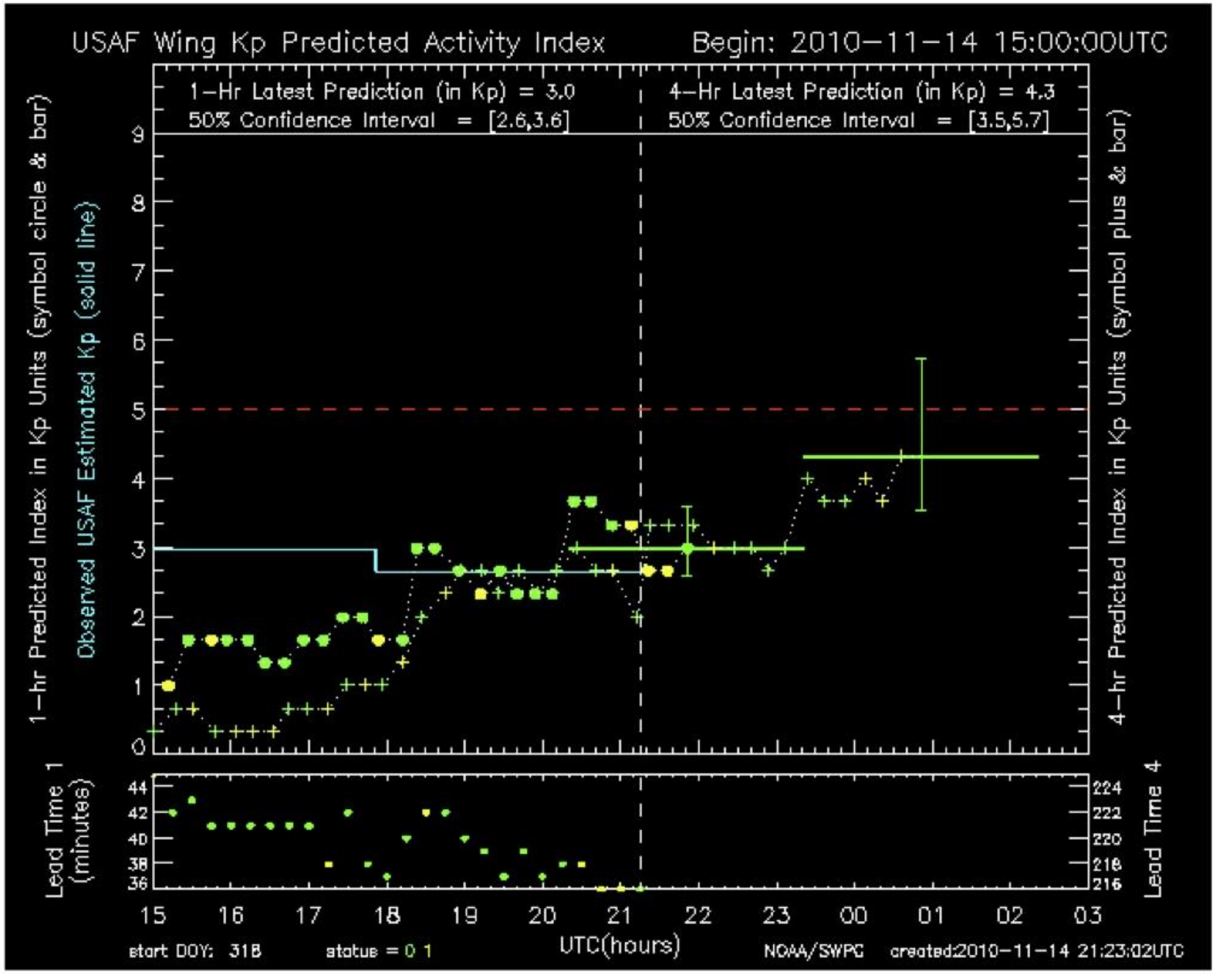


12-hour Plot -- 24-hour Plot -- ASCII list of model output -- 7 Day Model Performance

**Predictions update every 15 minutes**

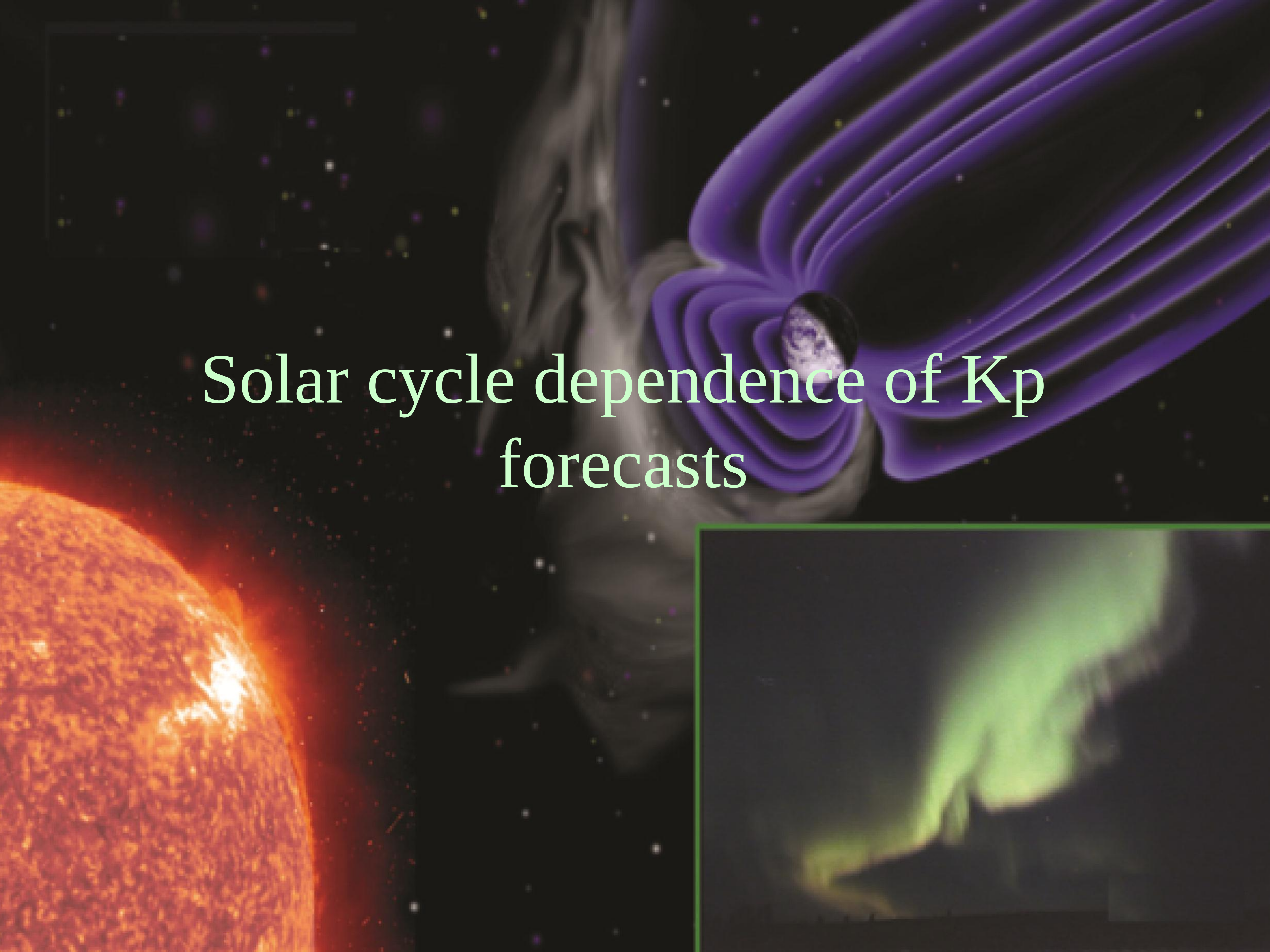

# Solar cycle dependence of Kp forecasts

# Kp (magnetospheric) predictability as a function of solar cycle

- Papitashvilli et al. [2000] reports that there is solar cycle variation in the average Kp.
- It would be interesting to determine if the accuracy of Kp (a proxy for the magnetospheric state) forecast based partly or entirely on solar wind/IMF has solar cycle dependence.
- Calculate the skill scores (TSS and GS [Detman and Joselyn, 1999]) for Kp forecast models for 2 solar cycles, 1975-2000.

# Kp predictability as a function of solar cycle

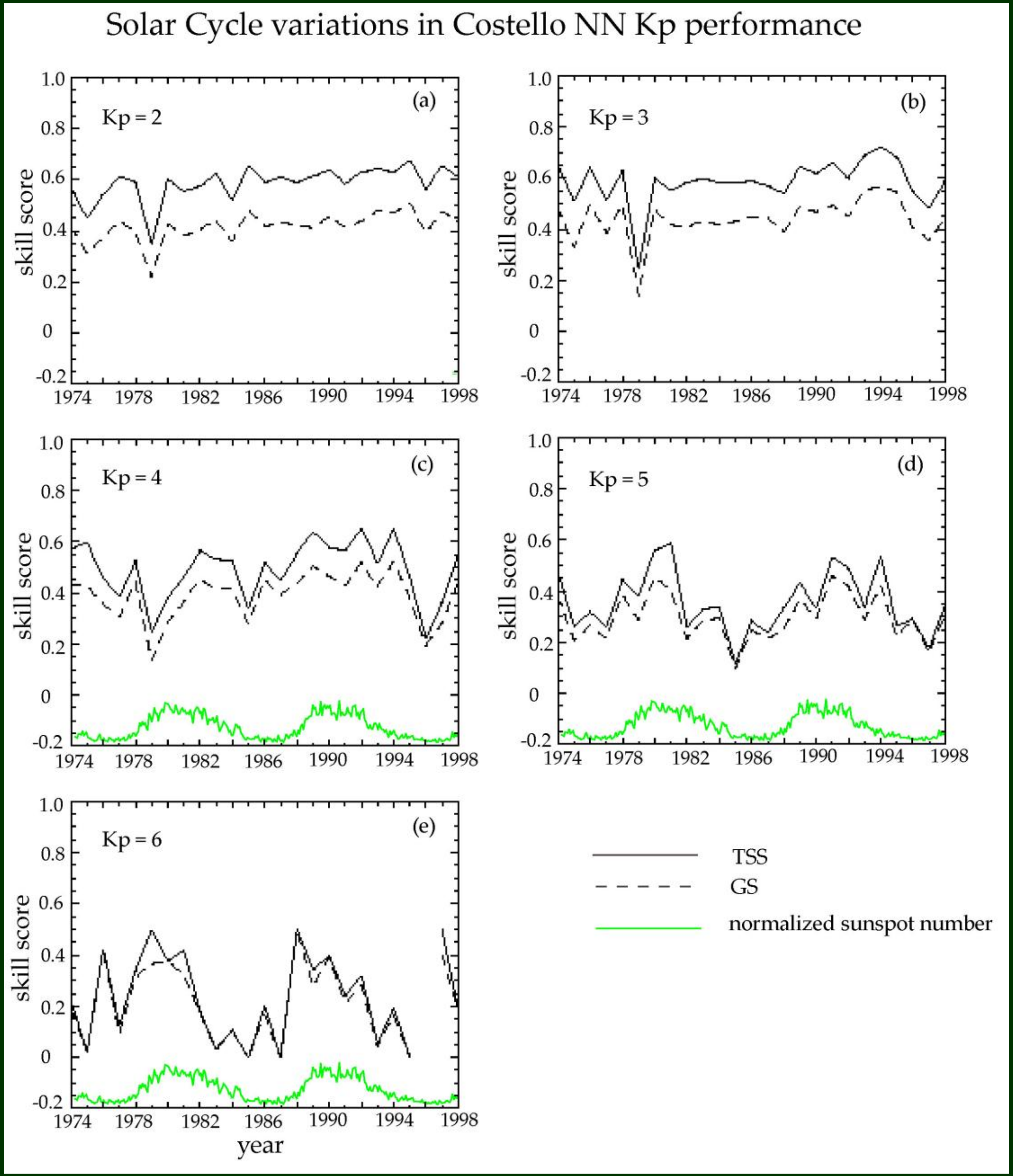


0 = random forecast
1 = perfect forecast

Costello NN Kp model predicts Kp more accurately near solar maximum than minimum.

# Kp predictability as a function of solar cycle

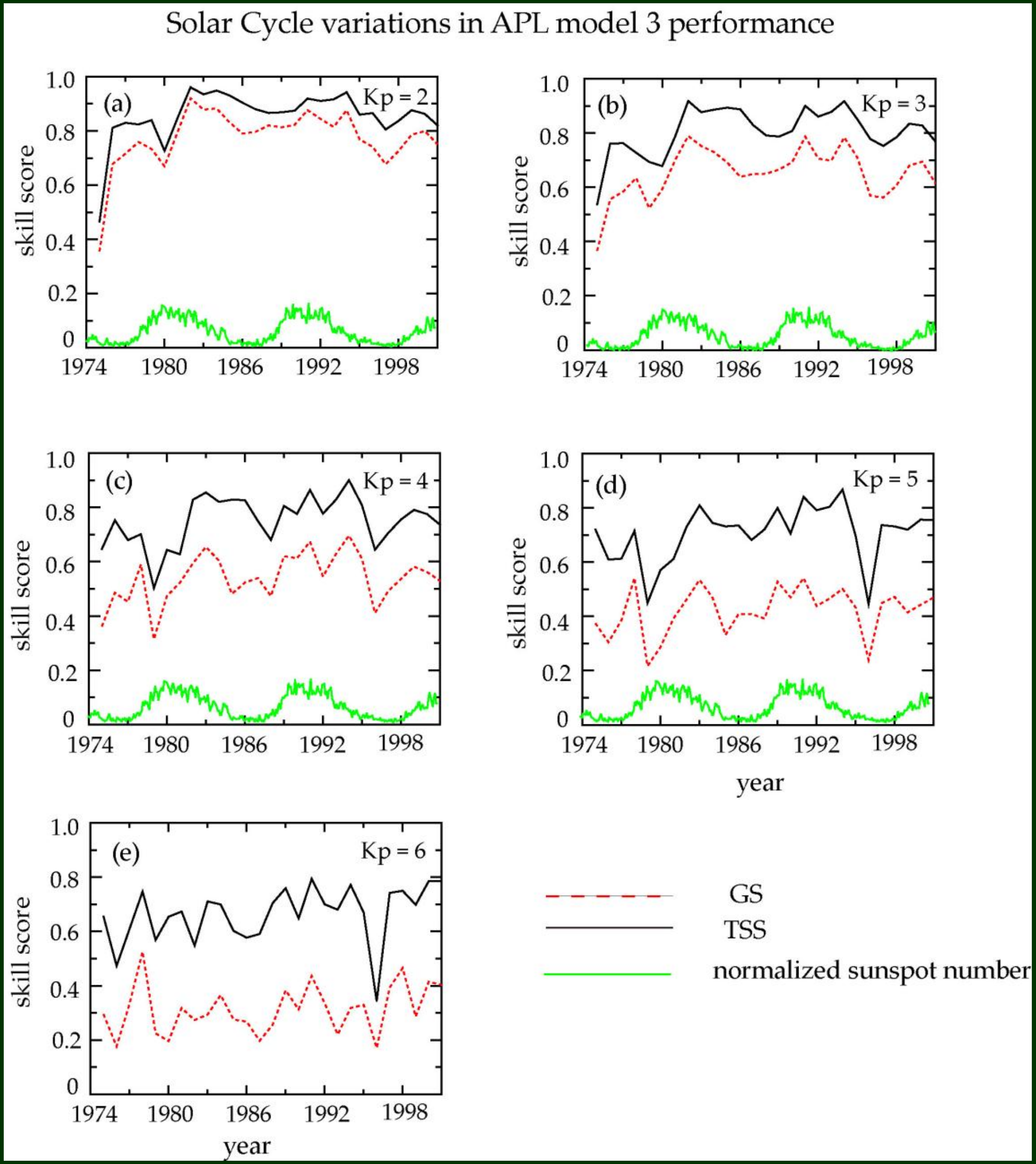


The solar cycle dependence of APL model 3

While the scores are higher than those for Costello model, they still exhibit solar cycle variation, albeit with smaller amplitude.

Training with a larger data set cannot eliminate the solar cycle effect completely.

APL model 3 performs better during solar max than solar min.

Wing et al. [2005][79]

# Kp predictability as a function of solar cycle

Solar minimum

Solar maximum

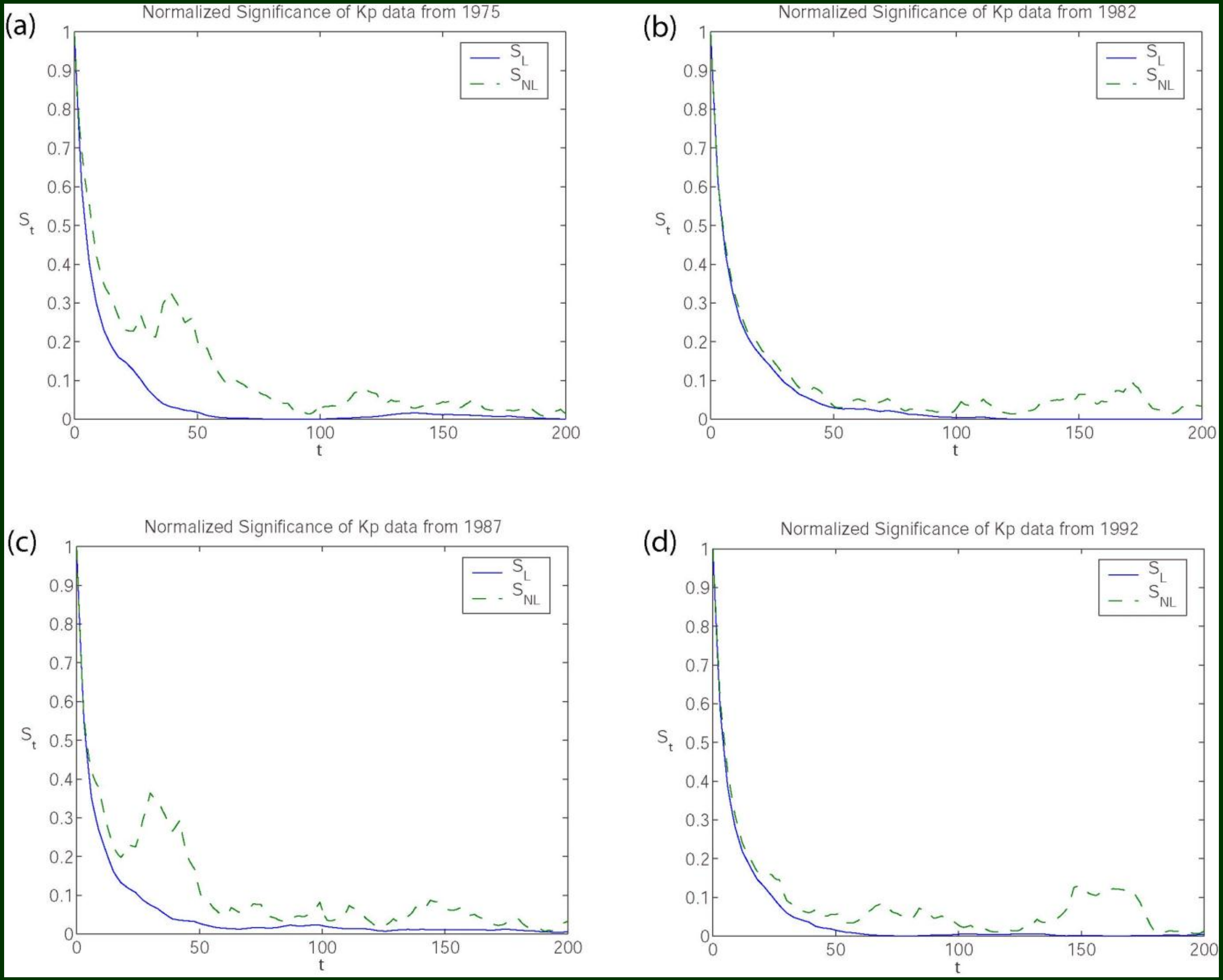


—— = $S_L$ ~ linear correlation [Kp(t), Kp(t - $\tau$)]

----- = $S_{NL}$ ~ nonlinear correlation

Cumulant based method analysis of the statistical informational dynamics of Kp time series.

The linear response is roughly equal, but the nonlinear response is stronger for solar min than solar max (peak ~ 40hr)

The magnetosphere is dominated more by internal dynamics during solar min than solar max, when it is more directly driven.

# Kp predictability as a function of solar cycle

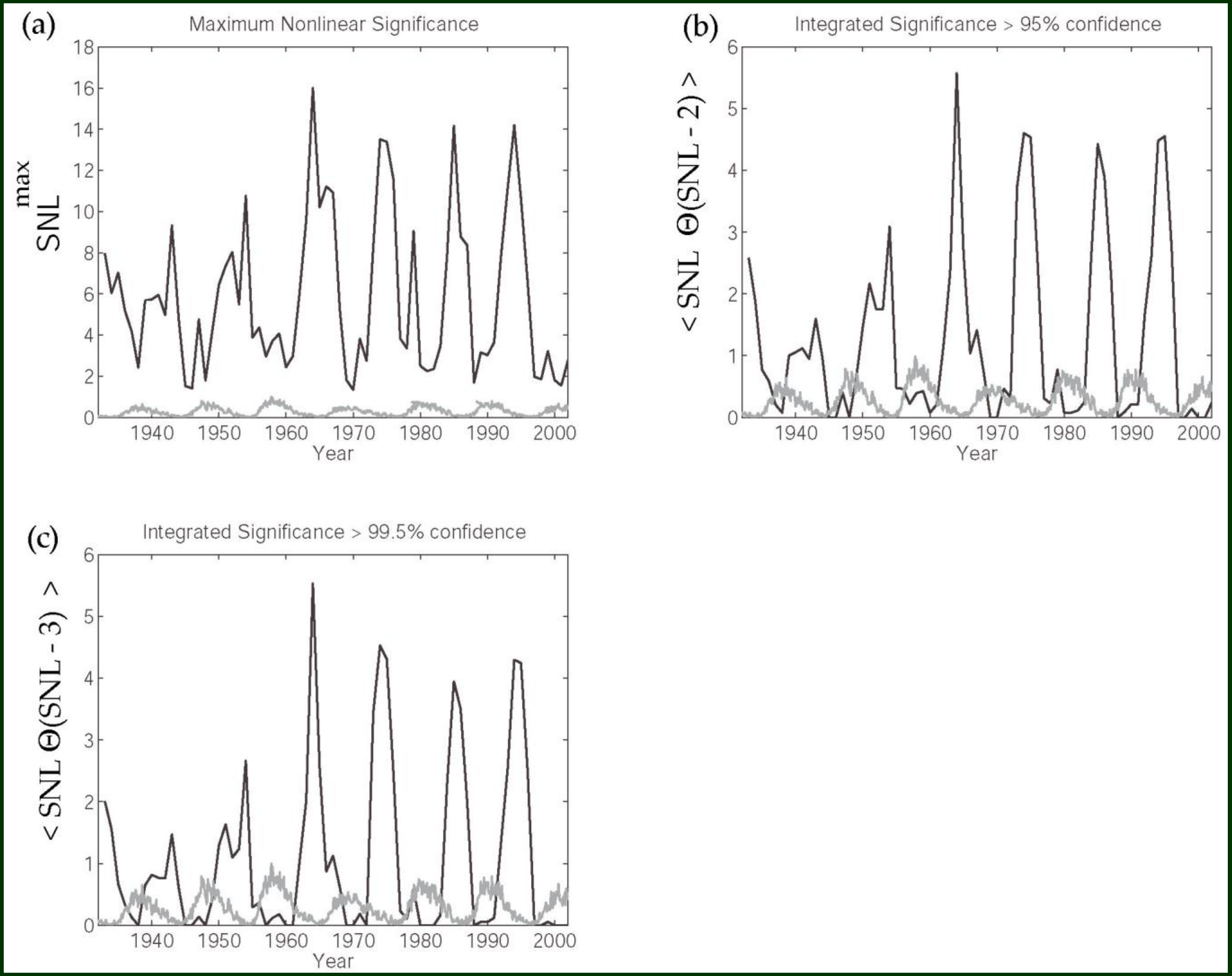


The nonlinear response anti-correlates with sunspot number in every solar cycle since Kp record is kept.

# The Nonlinearity is not Intrinsic to the Solar Wind

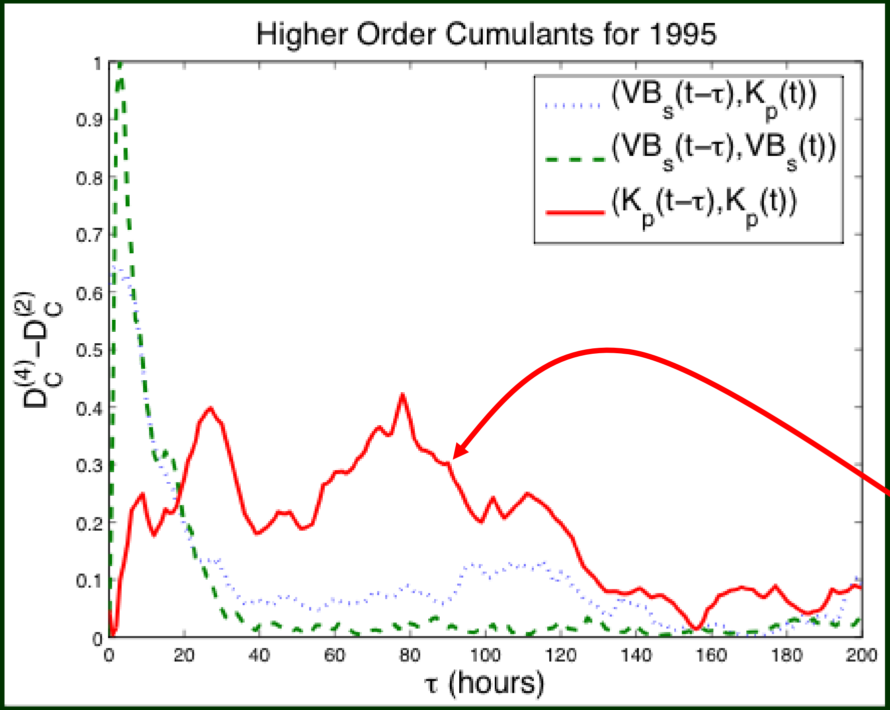


- Intrinsic solar wind nonlinearity maximizes at 2 hours delay and is small beyond 30 hours
- Kp peaks do not appear related to intrinsic solar wind nonlinearity
- Implication: the Kp nonlinearity is the result of internal dynamics

# 4. Summary

- Space Weather is relevant at high and low latitude (e.g., Indonesia)
  - can affect technologies and many daily activities
  - can affect Palapa satellites: communication and spacecraft charging
- Space weather at the equatorial region has not been as well understood as polar region → there is a lot of opportunities to make discoveries
- Ionospheric regions that disturb satellite communication:
  - high latitude scintillation: aurora particle precipitation
    - aurora dynamics
    - can affect intercontinental air travel
  - low latitude scintillation: plasma bubbles
    - has solar cycle and seasonal variations
    - TIMED GUVI and DMSP SSUSI
      - 2D plasma bubble images
      - 3D plasma density profiles
    - sometimes appear as “backward C” in 2D images

# 4. Summary

- Machine learning is a powerful tool for space weather forecasting
  - HF backscatters from ionospheric irregularities (clutters)
  - Kp forecast models
- Extensive Kp model evaluations based on data spanning over 2 solar cycles suggest that
  1. Kp is slightly more predictable during solar max than solar min.
  2. Cumulant based information dynamics analysis of Kp shows that Kp (the magnetosphere state) is more strongly nonlinearly coupled with the past Kps during solar min than solar max [Johnson and Wing, 2004].
  3. (1) and (2) suggest that the magnetosphere is more externally driven during solar max (declining phase of solar max) than solar min, when internal dynamics play a more significant role.


Thank you
2012 ISWI & MAGDAS